THE PENNSYLVANIA STATE UNIVERSITY
SCHREYER HONORS COLLEGE

DEPARTMENT OF BIOMEDICAL ENGINEERING

The Effect of Nanofiber Size and Orientation on Human Mesenchymal Stem Cell Nuclear Lamina Composition

ABBY GAYLE RIGGIO
SPRING 2021

A thesis
submitted in partial fulfillment
of the requirements
for a baccalaureate degree
in Biomedical Engineering
with honors in Biomedical Engineering

Reviewed and approved* by the following:

Justin Brown
Associate Professor of Biomedical Engineering
Thesis Supervisor and Honors Advisor

Daniel Hayes
Professor of Biomedical Engineering
Faculty Reader

* Electronic approvals are on file.

ABSTRACT

The field of tissue engineering seeks to apply stem cells to biocompatible scaffolds that allow for cell division and proliferation. Many characteristics and mechanical attributes of cells allow for successful division, especially the nuclear lamina, a fibrous network housed in the nucleus of a cell. Nuclear lamina regulate cellular division and provide mechanical support of cells. This is an imperative role in the realm of tissue engineering as laminas sense and respond to the specific mechanical properties of scaffolds such as elasticity and rigidity. Different scaffold size, orientation, or overall material compositions promote varying degrees of cellular adherence, division, and differentiation.

Human mesenchymal stem cells were applied to two different biocompatible nanofibers made of PMMA, a polymer, and one flat control surface. Primary and secondary antibodies were used as biomarkers for phosphorylated lamins within the nuclei and cytoplasm of the cells. Microscopy was then used to view immunostained phosphorylated stem cells on the different scaffolds to assess ideal scaffold conditions. CellProfiler was used to quantify the phosphorylated lamins of the applied stem cells. Phosphorylation within the lamins of the stem cells may imply successful proliferation on the scaffold as ongoing research shows nuclear lamina phosphorylation occurs at the onset of cellular division. It also may imply inhibition or promotion of cellular motility. The average cell and nuclei intensities varied greatly between the two fiber surfaces and the control surface within this study. The presence or absence of phosphorylated lamina as well as cellular and nuclei morphology can be used in a wide variety of applications in molecular research and in clinical settings.

TABLE OF CONTENTS

LIST OF FIGURES

LIST OF TABLES

ACKNOWLEDGEMENTS

I first would like to thank Dr. Justin Brown for his guidance, flexibility, and support especially through the pandemic. I have been able to learn so much through hands on experience in his musculoskeletal regenerative engineering laboratory and even more remotely with his help. I would also like to thank Dr. Daniel Hayes for acting as my faculty reader. Thank you to all the professors who have believed in me along the way.

Last, but not least, I would like to thank my incredible family. Thank you to my parents, who have given me an immense amount of love, support, and encouragement over the years. Thank you for listening to all my stress/excitement about school and for always believing in me. Thank you to my brother/role model who showed me the ways of engineering. I wouldn't be anyone without all of you.

Chapter 1

Background

Successful cellular division and differentiation are imperative for a stem cell to become a mature cell for use within the body. Stem cell engineering involves the application of stem cells onto biocompatible surfaces. These surfaces, or scaffolds, often drive stem cells to differentiate into a specific mature cell by mimicking the mechanical properties of the tissue or bone that the desired cell is found in. For example, if it is desired for a stem cell to become an adipocyte, a more elastic surface mimicking that of fat within the human body can help push the stem cell to become an adipocyte [1]. This is based on interactions between the cell and the surface they are applied to. Many properties of biological scaffolds impact cellular processes, especially division, of stem cells.

Stem Cell Characterization

Cells within the human body are characterized by their specific functions. For example, a white blood cell, or leukocyte, functions within the immune system. The basis of biology and the life sciences have taught that structure determines function. This carries over in the realm of biology on a cellular level as well. The different cell types in an organism have different structures that are better suited for their specific roles in the body. Thus, an immune system cell will look differently and serve a different purpose than a bone forming cell. Stem cells have changed the way that cells are characterized. Rather than being predetermined by a structure and function, stem cells are cells capable of differentiating into many different cell types. This has

opened a realm of research known as stem cell engineering that seeks to apply the more versatile nature of a stem cell in many applications such as to form tissues or potentially treat degenerative ailments. Scientists seek to "push" stem cells to differentiate into target cell types for various purposes specifically for regenerative medicine.

Stem cells are most notably characterized by their origin. Embryonic stem cells are taken from an embryo while it is in the blastocyst stage [1]. They are pluripotent, which means they can become any cell type [1]. Adult stem cells, often taken from bone marrow, are more limited in their differentiation possibilities and are most known to differentiate to blood cells, bone cells, or muscle cells [1]. Human mesenchymal cells (hMSCs) are multipotent stem cells meaning they are able to differentiate into cells within a certain class of cells, typically the mesodermal lineage [2]. These cell types are most often adipocytes or fat cells, osteocytes or bone cells, and chondrocytes or cartilage cells [2].

Cellular Division Phosphorylation

The cell cycle includes many notable checkpoints that a cell must reach in order to begin to divide. Cells are often in the growth phases of the cycle, but when they are ready to divide somatic cellular division begins the process of mitosis. Cellular division is a highly regulated process that is necessary within an organism for growth and repair. During division, cells must undergo a series of structural and chemical changes initiated by biochemical agents, specifically cyclin-dependent kinases [3]. Cyclin-dependent kinases are biological catalysts that initiate the phosphorylation of molecules by transferring a phosphate group from a readily available ATP molecule [3]. Phosphorylation is a common cellular process that changes the structure of the

targeted molecule, which in turn can either inhibit or activate the specific molecule's function [3]. In cellular division, phosphorylation is responsible for many events such as the condensation of chromosomes and the breakdown of the nuclear envelope [4]. The nuclear lamina specifically undergoes phosphorylation in different ways during mitosis.

The Nuclear Lamina

The nuclear lamina is a fibrous structure within the inner wall of the nucleus of cells made up of type V intermediate filaments called lamins [5]. There are many different classes of lamins that create the overall structure of the nuclear lamina such as: lamin A, lamin C, lamin C2, lamin B1, and more [5]. Lamin A is believed to be only found in differentiated cells but may be present in stem cells as well [6]. B-type lamins are needed for organogenesis and are thus more widespread and found in all developing cells [6]. Lamin A/C possess lamin-binding abilities in their tail domain [6]. These binding domains allow for structural changes in many forms including assembly of a lamin network [6]. Mutations within this tail domain can lead to many altered functions such as poor lamin assembly, lower nuclear stiffness, or impairment in mechanosensitive genes, which in turn can affect gene expression [6]. Many of the structural changes that nuclear lamina undergo can either inhibit or promote downstream changes in the nucleus, in neighboring cells, or in cell-surface interactions. As structure determines function as noted earlier, any change to the overall structure of the lamin will affect how it performs its duties within the cell.

Phosphorylation of Lamins

The process of phosphorylation, the addition of a phosphate group, interferes with the organization of the nuclear lamina meshwork [6]. As the organization changes, the material properties of the nuclear lamina changes in terms of characteristics like stiffness, deformability, etc. [6]. Figure 1 shows a nuclear pore, a small opening within the nucleus, as well as nuclear lamina within the inner membrane of the nucleus.

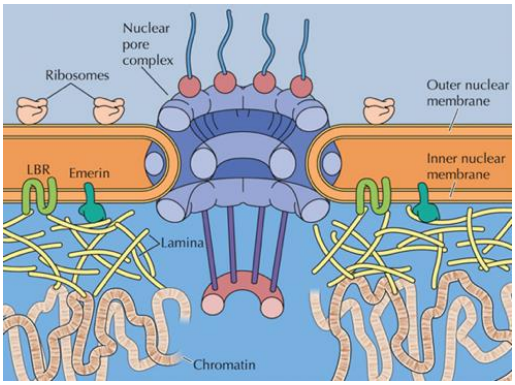

Figure 1. Nuclear membrane depicting nuclear lamina through a nuclear pore [7]

Lamin A most commonly undergoes post-translational phosphorylation [8]. This phosphorylation is most evident during interphase and mitosis during the cell cycle but is not very well understood [8]. Most research into the phosphorylation of nuclear lamina has looked at assembly and disassembly [8]. Disassembly of lamina must occur in order for mitotic spindles to attach to the chromosomes at the metaphase plate [6,8]. The lamins will then re-assemble following cellular division. The phosphorylation during mitosis is known to be facilitated by cyclin dependent kinase 1 (Cdk1) [8]. However, Cdk1 appears to only phosphorylate the N-terminus of human lamin A, which may not be enough to promote disassembly [8]. This may mean another Cdk in conjunction with Cdk1 is responsible for the overall disassembly process [8]. The following figure shows the disassembled and assembled lamina.

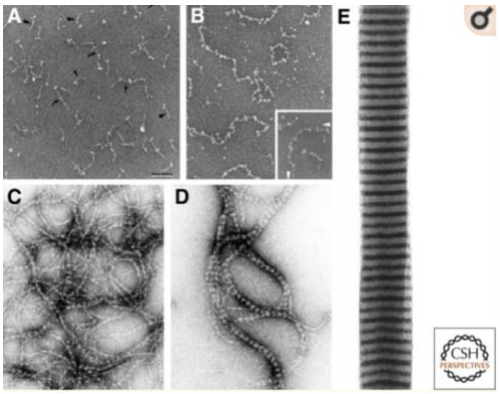

Figure 2. Assembly process of nuclear lamina. a) dimers formed b) dimers come together c) more assembly "beadlike" d) thick organized fibers e) helical wound arrays [9]

The filaments will eventually assemble into array like formation as seen in figure2.e [9]. This high ordered structure of assembly appears as a tightly wound coil like structure that occurs as the lamina assembles head-to-tail [9]. Lamina may take this form at the completion of cell division as initiated by de-phosphorylation events [9].

This entire process of phosphorylation and de-phosphorylation of nuclear lamina plays a large role in stem cell-surface interactions at the molecular level. Recent studies have learned that lamins act as mechanosensors to their surroundings [8]. This cell-signaling is imperative in stem cell engineering applications. A domino effect occurs because of the sensing abilities. Surface stiffness impacts lamina phosphorylation, which in turn affects overall nuclear stiffness and cell motility [8]. This cell signaling idea can be seen below in figure 3 depicting how the input, stiffness in this case, affects the lamina, which in turn have many other impacts on the cell as a whole such as transcription of DNA to mRNA [8]. This chain of events may be helpful in understanding the ideal surface properties needed for successful regenerative medicine.

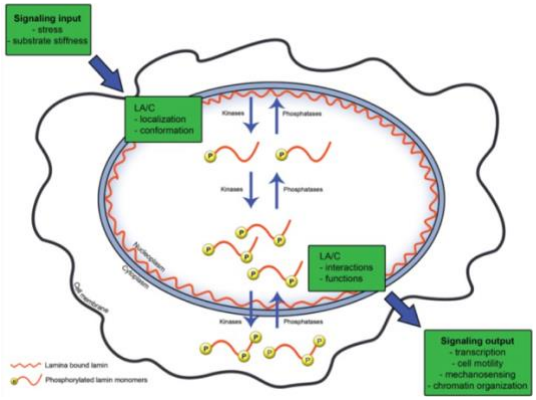

Figure 3. Impact that the cellular environment properties such as stiffness have on phosphorylation of nuclear lamina and the impact of phosphorylated lamina have downstream in the cell [8]

Localization of Phosphorylated Lamins

Phosphorylation of the lamin A/C type can also impact the localization of the lamin itself [8]. Although research is ongoing for this phenomenon, it was found that phosphorylation can determine which lamin type is present in the nucleus or in the cytoplasm of the cell [8]. Once cellular division progresses and the nuclear envelope breaks down, phosphorylated, disassembled, lamin A/C are abundantly dispersed throughout the cytoplasm [10]. As cellular division comes to a close near the end of telophase, lamin A/C accumulate and are likely dephosphorylated [10].

Biocompatible Scaffold Techniques

Stem cells are typically introduced to biological surfaces and scaffolds. These scaffolds provide a rough framework of the desired shape of desired cellular growth. In general, a successful scaffold or surface in stem cell engineering is one that is biocompatible, capable of degradation, and possesses the desired mechanical properties [11]. Biocompatibility is arguably

the most important factor because the surface must promote cellular growth [11]. The scaffold also must be able to degrade as needed after the cells have proliferated, but not too soon into the growth process either [11]. Electrospinning is one of the most common techniques in creating biocompatible scaffolds for tissue engineering. The process of electrospinning involves ejecting melted polymer to form very fine fibers in a desired two-dimensional shape [12]. The fibers often resemble small threads crossing over one another creating a meshwork with voids [12]. The resulting surfaces are nanofibers that can be manipulated into three dimensional geometries [12]. The high surface-area-to-volume meshwork of fibrous scaffolds are ideal in stem cell engineering because cells are able to spread within the voids [12]. The electrospinning process and device can be seen below in the simplified diagram.

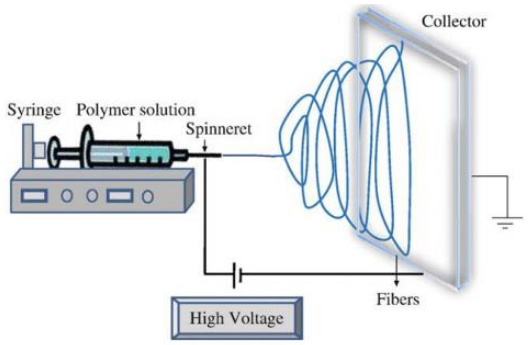

Figure 4. Electrospinning apparatus depicting spinning of the growing polymer ejected from the spinneret and collected on a collecting plate [13]

Cellular Orientation on Nanofiber Meshworks

There have been many different studies into the way that stem cells adhere to nanofiber surfaces. The intricate network of nanofibers closely resembles the extracellular matrix (ECM) that surrounds cells within the human body. Because of this mimicry, cells interact and anchor to the nanofibers similarly to how they would within the ECM [14].

One study completed looked at the geometric potential theory and how it can be used to model the interactions between nanofibers and cells [14]. The geometric potential theory discusses that boundaries create forces that are normal to the surface of the boundary itself [14]. These forces can be related to Earth's gravity because gravity acts perpendicular to the surface of the Earth [14]. On a much smaller level, these perpendicular forces can be attributed to capillary action as water moves up small capillaries [14]. As distance increases between two boundaries, the geometric potential becomes weaker [14]. This is important in cell-nanofiber interactions because as nanofiber distance increases, cell interactions may change or decrease [14]. Similar to how water can "crawl" against gravity when capillary action is occurring, a cell can attach to parallel fibers, wrap around them to anchor itself, and then spread upwards as if it is "crawling" [14]. Figure 5 below shows this cell spreading phenomenon. This cell spreading can be modeled mathematically by the geometric potential theory as well.

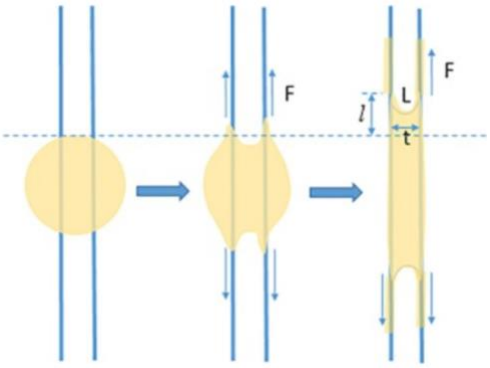

Figure 5. Parallel fiber stem cell spreading [14]

This cellular spreading eventually can lead to neighboring cells interaction with one another as well [14]. This can lead to new tissue formation, which is often the desired result of stem cell engineering research.

The specific type of nanofiber can also dictate how a cell will interact with the biocompatible surface. Poly(methyl methacrylate) or PMMA is a synthetic plastic-like polymer

commonly known as Plexiglass [15]. It is commonly used to create nanofiber scaffolds and was used to create the nanofibers in this thesis, which will be further discussed later [15]. PMMA is often dissolved in a solvent like acetone to form a solution that can be inserted into the electrospinning device for fiber creation [15]. These electrospun fibers are rigid and highly biocompatible [15]. Stem cells are often applied to these surfaces because of these suitable characteristics [15]. Figure 6 below shows results from a previous study by Ura et al of cells interacting with both PMMA nanofibers and PMMA microfibers [15]. Filopodia, which are small cellular membrane protrusions, interact with surrounding surfaces as seen below [15]. These help provide support and anchor the cells to the fibers. They appear as small arm-like projections that are able to wrap around the rod-shaped fibers [15]. Once anchored, stem cells will begin to stretch to cover a larger surface area and to communicate with neighboring cells [15].

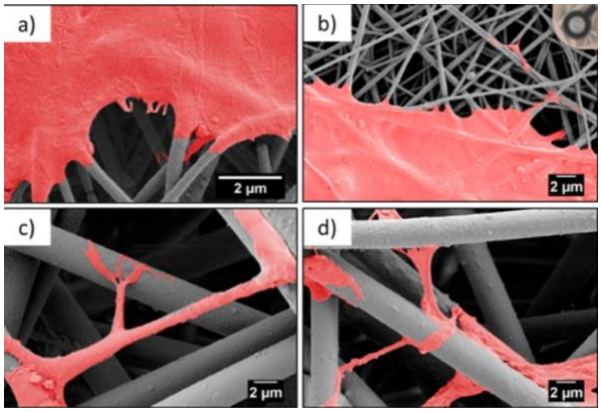

Figure 6. Stem Cell Interactions with Nanofibers (a,b) and Microfibers (c,d) [15]

Many cell-fiber interactions dictate the overall success of stem cell engineering. These are driven by many molecular mechanisms, cellular structures, and material properties of scaffolds. These considerations and prior studies were kept in mind when completing the

research for this thesis. In order to better understand the roles that nuclear lamina play in both cell motility and in the overall stem cell engineering process, human mesenchymal stem cells and their nuclear lamina were studied on various surface types. It was hypothesized that there would be a statistical significance between the average cell and nuclei intensities of phosphorylated lamin A/C between each of the three surfaces. This was based on prior studies and the importance of mechano-sensing of the nuclear lamina.

Chapter 2

Methods

Similar procedures completed in the studies above were followed for the experimental protocol in this thesis. hMSCs were cultured and applied to various surface types. Primary and secondary antibodies were used to tag phosphorylated lamina in these cells as they grew over their surfaces. The average intensities of phosphorylated lamina in the nucleus and in the cytoplasm of these cells were found using various software such as CellProfiler. This data was then subject to statistical testing to determine statistical significance between the mean intensities. A more detailed account of the overall procedure is discussed below.

Cell Culture

Human mesenchymal stem cells (hMSCs) were first thawed by slowly turning the frozen vial in a warm water bath. The thawed cells were then plated with bovine serum media (Minimum Essential Medium, Alpha 1X with Earle's salts, ribonucleosides, deoxyribonucleosides & L-glutamine, 10% FBS, 15 P/S) for growth. For medium size plates,

approximately 10 mL of media was added to one vial of thawed cells. The plates were labeled and placed in an incubator set at 37 °C, the average human body temperature. The media in each plate was changed every couple of days to ensure that cells had adequate nutrients at all times. Figure 7 shows cells on plates with media under light microscopy.

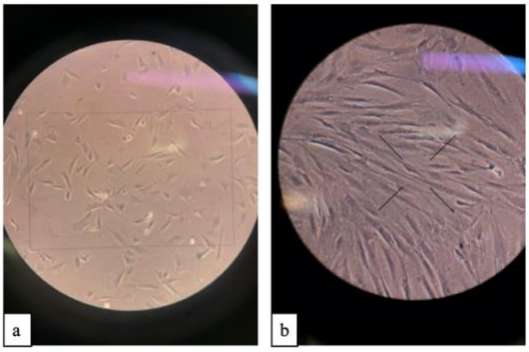

Figure 7. hMSCs in culture under light microscopy after a) initial growth b) after widespread growth before splitting

The cells were transferred to larger plates, or split, as needed. This was done by applying a small amount, typically 2 mL, of trypsin to each plate. Trypsin breaks down proteins that anchor the stem cells to the surface of the plate. After the cells sat in tryspin for approximately 3-5 minutes, the cells released from the plate and were then in suspension. These cells could then be easily transferred to new plates via simple pipetting. New media was then added and changed every couple of days like before.

Creation of Surfaces

Three surfaces were used in this study: a flat control surface and two different PMMA fibers. PMMA is often purchased in powder form and dissolved in a solvent before use. Two different types of surfaces made from PMMA were created with differing diameters to assess

which diameter led to more nuclear lamina phosphorylation. The first PMMA nanofiber surfaces were created of 5% PMMA in the solvent of 2,2,2-Trifluoroethanol (TFE). This yielded a thinner meshwork of fibers approximately one micron in diameter. The second PMMA nanofiber surfaces were created of 10% PMMA also dissolved in the solvent of TFE. This yielded a thicker meshwork of fibers approximately two microns in diameter. Once the PMMA was dissolved, the solution was inserted into the electrospinning apparatus' syringe. A voltage of 15,000 V was applied, which slowly pushed the polymer through the needle of the syringe called the Taylor cone. The polymer then became solid and spun quickly as it exited the cone onto the collecting plate located 15 cm away. The result was small electrospun fibrous scaffolds. Figure 8 below shows the 5% PMMA nanofibers and adhered cells, while figure 7 shows the 10% PMMA nanofibers and adhered cells. Both images below were taken via DIC.

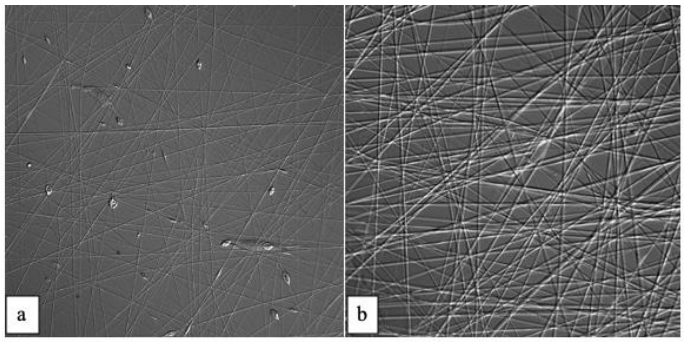

Figure 8. PMMA nanofibers with live cells adhered under DIC with approximate diameters of a) one micron b) two microns

The control surface was simply a flat surface that the cells grew and divided on. hMSCs were suspended in their culture and then added to these three different surfaces. Everything other than surface type, such as incubation temperature (37 °C), was kept constant to remove any extraneous error.

Use of Antibody Labeling

Antibody labeling or immunolabeling is a method used in biomedical research to label structures of interest [16]. There are two distinct techniques of antibody labeling: direct and indirect [16]. Direct uses only primary antibodies, while indirect uses both primary and secondary antibodies [16]. Indirect immunofluorescence techniques were used in this study because the use of secondary antibodies typically amplifies the intensity of the structure of interest [16].

Primary antibodies are protein bound specific, which means their primary role is to bind to the structure of interest [16]. Secondary antibodies are polyclonal, typically in the class of IgG, and are species specific [16]. Secondary antibodies bind to the bound primary antibody and amplify the fluoresce of the dye thus labeling the structure desired. Primary and secondary antibodies, Phospho-Lamin A/C (Ser22) Antibody #2026, were purchased from Cell Signaling Inc. [17]. These antibodies were supplied in 10 mM sodium HEPES (pH 7.5), 150 mM NaCl, 100 ug/mml BSA, and 50% glycerol [17]. They are stored at -20 °C until applied to cells [17]. They are diluted 1:800 when used in immunofluorescence applications such as this study [17]. They are reactive with human, mouse, and rat cell lines and detect lamin A/C when they are phosphorylated at the Ser22 residue [17]. This phosphorylation site is studied because the sequence following is a signal pathway that serves a role in cellular division [17].

Alexa Fluor 568 dye, an orange-fluorescent dye, was used to label channel 00, the channel corresponding to the laminas [18]. Alexa Fluor 488 dye, a green-fluorescent dye, was used to label channel 01, the channel corresponding to pLam or phosphorylated laminas [19]. Alexa 350 phalloidin, a blue- fluorescent dye, was used to label channel 02, the channel

corresponding to actin [20]. This dye was chosen because it "selectively stains F-actin" [20]. Each dye fluoresces at a different wavelength corresponding to the number in each dye name.

Application of Antibodies to Cells

Once the cells were thawed and placed in media on their surfaces, the labeling antibodies were prepared and added. Cells are typically washed with PBS before addition of immunostaining occurs. The general methods to immunostaining follow a strict procedure as outlined by the manufacturer. The manufacturer often provides instructions for ideal use of their antibodies. The following procedural steps are courtesy of CellSignaling Inc., the company that these specific antibodies were purchased from [17]:

NOTE: Prepare solutions with reverse osmosis deionized (RODI) or equivalent grade water.

1. **20X Phosphate Buffered Saline (PBS):** (9808) To prepare 1L 1X PBS: add 50 ml 20X PBS to 950 ml dH_2O, mix. Adjust pH to 8.0.
2. **Formaldehyde**: 16%, methanol free, Polysciences, Inc. (cat# 18814), use fresh and store opened vials at 4°C in dark, dilute in 1X PBS for use.
3. **Blocking Buffer** (1X PBS / 5% normal serum / 0.3% Triton™ X-100): To prepare 10 ml, add 0.5 ml normal serum from the same species as the secondary antibody (e.g., Normal Goat Serum (#5425)) and 0.5 mL 20X PBS to 9.0 mL dH_2O, mix well. While stirring, add 30 µl Triton™ X-100.
4. **Antibody Dilution Buffer** (1X PBS / 1% BSA / 0.3% Triton X-100): To prepare 10 ml, add 30 µl Triton™ X-100 to 10 ml 1X PBS. Mix well then add 0.1 g BSA (9998), mix.

1. B. Specimen Preparation - Cultured Cell Lines (IF-IC)

NOTE: Cells should be grown, treated, fixed and stained directly in multi-well plates, chamber slides or on coverslips.

2. Aspirate liquid, then cover cells to a depth of 2–3 mm with 4% formaldehyde diluted in 1X PBS.
3. Allow cells to fix for 15 min at room temperature.
4. Aspirate fixative, rinse three times in 1X PBS for 5 min each.
5. Proceed with Immunostaining (Section C).
6. C. Immunostaining

NOTE: All subsequent incubations should be carried out at room temperature unless otherwise noted in a humid light-tight box or covered dish/plate to prevent drying and fluorochrome fading.

1. Block specimen in Blocking Buffer for 60 min.
2. While blocking, prepare primary antibody by diluting as indicated on product webpage in Antibody Dilution Buffer.
3. Aspirate blocking solution, apply diluted primary antibody.
4. Incubate overnight at 4°C.
5. Rinse three times in 1X PBS for 5 min each.
6. Incubate specimen in fluorochrome-conjugated secondary antibody diluted in Antibody Dilution Buffer for 1–2 hr at room temperature in the dark.
7. Rinse three times in 1X PBS for 5 min each.
8. Coverslip slides with Prolong® Gold Antifade Reagent (#9071) or Prolong® Gold Antifade Reagent with DAPI (#8961).

9. For best results, allow mountant to cure overnight at room temperature. For long-term storage, store slides flat at 4°C protected from light.

Imaging

Images were taken of each surface in different locations to analyze intensities of the biomarker antibodies. Eighteen sets of images were taken from the flat control surfaces. Eighteen sets of images were taken from different locations on the 5% PMMA surfaces. Fifteen sets of images were taken from different locations on the 10% PMMA surfaces. These image sets were then inputted into CellProfiler for quantification.

CellProfiler Use

CellProfiler is a software used to quantify and visualize cells based on python, a programming language. It utilizes pipelines that each play specific roles as needed by the researcher. Each pipeline is used to outline images/objects, count objects/images, etc. For this experiment the following pipelines were used: identifyprimaryobjects, identifysecondaryobjects, measureobjectintensity, and measureobjectsizeshape.

Identifyprimaryobjects was used to identify the nuclei in the lamin channel 00 images. Identifysecondaryobjects was used to identify the cells in the actin channel 02. The identification of objects is often image specific. Three channels (00, 01, 02) of one image were inputted. The threshold values within the identifysecondaryobjects pipeline were changed as needed in CellProfiler. The measureobjectintensity pipeline was used to measure the fluoresced intensities of nuclei and cells for the phosphorylated lamina images (channel 01). These pipelines allowed

for easy identification of cells that possessed phosphorylated lamina in both the cytoplasm and nucleus of the cells. Measureobjectsizeshape provided cell and nuclei morphology data. The CellProfiler interface and the pipelines used can be seen below in figure 9.

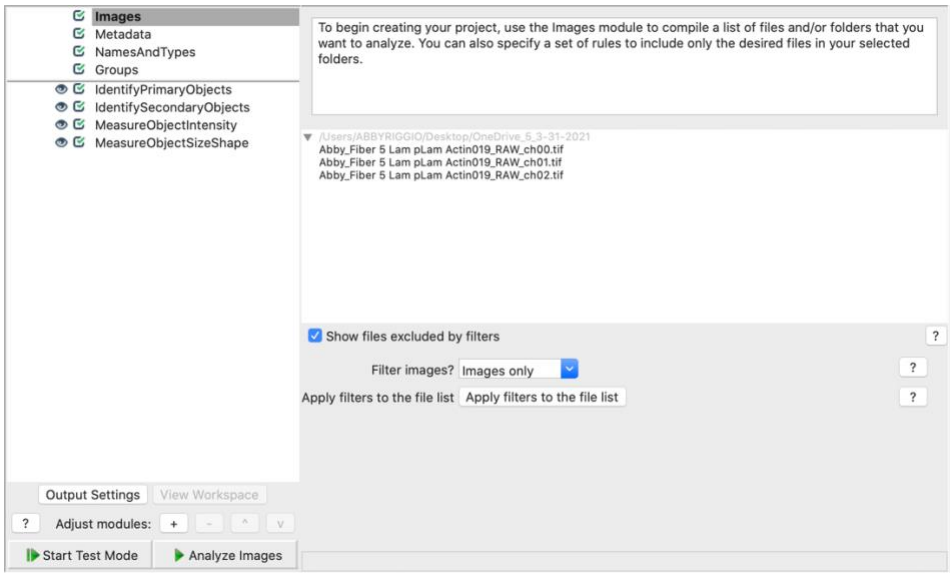

Figure 9. CellProfiler interface depicting used pipelines

The left of figure 9 shows the added four pipelines used to a) identify the fluoresced nuclear lamin, b) identify the fluoresced cytoplasmic lamin, c) quantify the intensities of the fluoresced objects, and d) measure cell and nuclei morphology. Images are uploaded to image section of the sidebar and are grouped based on name in the groups section of the sidebar.

ImageJ Use

ImageJ is another software used in biomedical research. It is an imaging software that can correct color scales, overlay images, etc. ImageJ was used in this research to better visualize the images of each channel. It was also used to improve the contrast of the DIC images taken,

labeled as channel 03. These images can be found in Appendix B. ImageJ was also used to confirm the approximate width of the created nanofibers. Once an image of the fiber surface was uploaded to ImageJ, a line was drawn over the width of a visible fiber. Under the analyze heading, plot profile was selected. This then displayed a graph depicting two peaks. The estimated distance from one peak to the other yielded the estimate of the fiber diameters.

Statistical Testing

T-tests are statistical tests that determine significance between two means. This type of test was used to better understand if the average intensities on one surface type were significant with respect to the average intensities found on another. These were also used to determine any significance between aspect ratios of the cells and nuclei on different surfaces. This statistical testing was done by using the data analysis tools embedded in Microsoft Excel. The chosen tests performed were the following: t-Test two-sample assuming unequal variances. This type of t-test was chosen because the variances in each image set were very different from one another.

Chapter 3

Results

Object Identification

The following object identification results were obtained from the identifyprimaryobjects and identifysecondaryobjects pipelines in CellProfiler. One example for each of the surfaces can be seen below. The remaining object identification images can be found Appendix A.

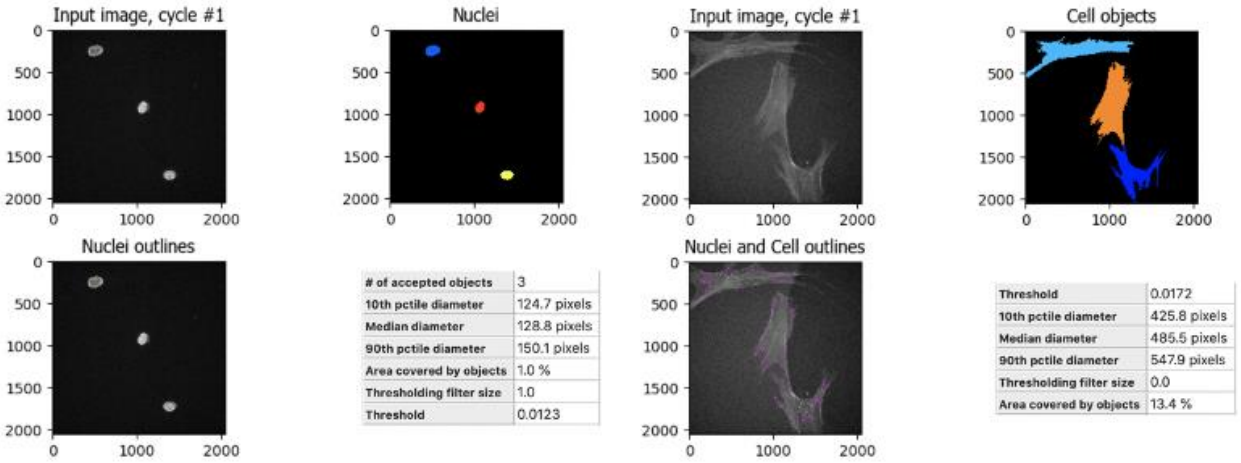

# of accepted objects	3
10th pctile diameter	124.7 pixels
Median diameter	128.8 pixels
90th pctile diameter	150.1 pixels
Area covered by objects	1.0 %
Thresholding filter size	1.0
Threshold	0.0123

Threshold	0.0172
10th pctile diameter	425.8 pixels
Median diameter	485.5 pixels
90th pctile diameter	547.9 pixels
Thresholding filter size	0.0
Area covered by objects	13.4 %

Figure 10. Nuclei and cells identified on flat control surface using CellProfiler

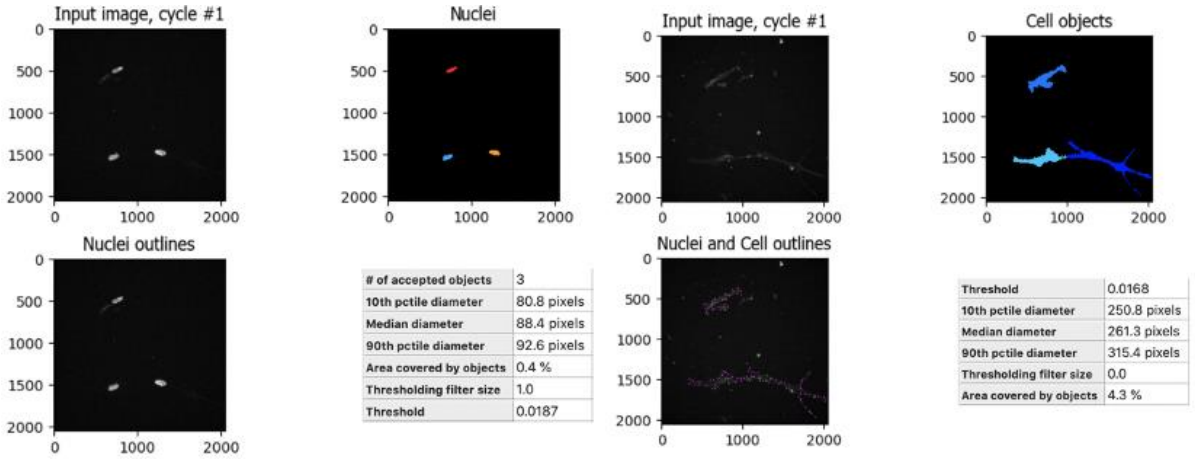

# of accepted objects	3
10th pctile diameter	80.8 pixels
Median diameter	88.4 pixels
90th pctile diameter	92.6 pixels
Area covered by objects	0.4 %
Thresholding filter size	1.0
Threshold	0.0187

Threshold	0.0168
10th pctile diameter	250.8 pixels
Median diameter	261.3 pixels
90th pctile diameter	315.4 pixels
Thresholding filter size	0.0
Area covered by objects	4.3 %

Figure 11. Nuclei and cells identified on 5% PMMA surface using CellProfiler

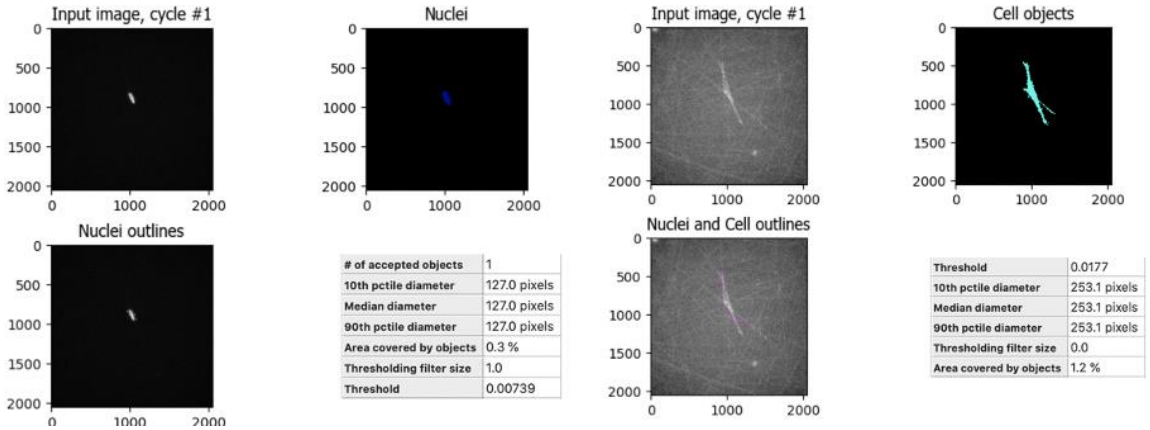

# of accepted objects	1
10th pctile diameter	127.0 pixels
Median diameter	127.0 pixels
90th pctile diameter	127.0 pixels
Area covered by objects	0.3 %
Thresholding filter size	1.0
Threshold	0.00739

Threshold	0.0177
10th pctile diameter	253.1 pixels
Median diameter	253.1 pixels
90th pctile diameter	253.1 pixels
Thresholding filter size	0.0
Area covered by objects	1.2 %

Figure 12. Nuclei and cells identified on 10% PMMA surface using CellProfiler

Phosphorylation Intensities

Measureobjectintensity pipeline was used in conjunction with these identified objects to determine overall phosphorylation. Figure 13 shows an example portion of the measureobjectintensity window for the control surface cells image 2. This window lists intensities as needed for both the cell (pictured) and nuclei (not pictured).

Image	Object	Feature	Mean	Median	STD
pLam	Cell	IntegratedIntensity	1121.494	1121.494	179.649
pLam	Cell	MeanIntensity	0.017	0.017	0.001
pLam	Cell	StdIntensity	0.002	0.002	0.0
pLam	Cell	MinIntensity	0.011	0.011	0.0
pLam	Cell	MaxIntensity	0.031	0.031	0.004
pLam	Cell	IntegratedIntensityEdge	62.161	62.161	0.868
pLam	Cell	MeanIntensityEdge	0.016	0.016	0.0
pLam	Cell	StdIntensityEdge	0.001	0.001	0.0
pLam	Cell	MinIntensityEdge	0.012	0.012	0.0
pLam	Cell	MaxIntensityEdge	0.027	0.027	0.008
pLam	Cell	MassDisplacement	3.882	3.882	0.274
pLam	Cell	LowerQuartileIntensity	0.015	0.015	0.0

Figure 13. CellProfiler measureobjectintensity window example for image 2 of control surface cells

Three channel images represented one location on each surface. For each set of these images, an average integrated cell and nuclei intensity was found. The compiled results of integrated intensities for each image set within each surface can be found in the following tables. Table 1 lists the average intensities on each flat control surface location. Table 2 lists the average intensities for the cell and nuclei at each location on the 5% PMMA surface. Table 3 lists the average intensities for the cell and nuclei at each location on the 10% PMMA surface. These values were compared and inputted into several t-tests to determine statistical significance.

Table 1. Integrated cell and nuclei intensities in pLam channel for flat control surfaces

Image Number	Integrated Cell Intensity Average	Integrated Cell Intensity Median	Standard Deviation Integrated Cell Intensity	Integrated Nuclei Intensity Average	Integrated Nuclei Intensity Average	Standard Deviation Integrated Nuclei Intensity
2	1121.494	1121.494	179.649	163.262	163.262	1.258
3	2930.462	2930.462	1308.331	333.233	333.233	40.138
4	2814.795	2939.518	691.674	247.704	254.507	21.724
5	8513.149	8513.149	0	417.81	417.81	0
6	6910.054	6910.054	6707.421	262.645	262.645	61.665
7	4113.011	4113.011	3623.313	225.169	225.169	72.946
8	9238.82	9238.82	0	240.174	240.174	0
9	3114.856	3114.856	257.662	308.04	308.04	20.795
10	2525.305	2525.305	743.56	241.779	241.779	43.188
11	3510.095	3510.095	334.311	286.952	286.952	38.253
12	2041.092	2041.092	629.933	186.613	186.613	9.566
13	3504.761	2981.662	752.718	286.096	260.639	15.278
14	2671.821	2671.821	294.287	261.959	261.959	62.132
15	2884.851	2711.593	624.979	258.76	247.063	25.106
16	3082.97	3472.299	1522.231	252.529	257.434	40.017
17	4074.31	2635.688	2778.413	287.804	205.542	136.012
18	3989.203	4870.078	2115.66	221.652	224.431	48.885
19	2651.277	2900.625	2460.674	262.956	267.125	65.077

Table 2. Integrated cell and nuclei intensities in pLam channel for 5% PMMA surfaces

Image Number	Integrated Cell Intensity Average	Integrated Cell Intensity Median	Standard Deviation Integrated Cell Intensity	Integrated Nuclei Intensity Average	Integrated Nuclei Intensity Average	Standard Deviation Integrated Nuclei Intensity
1	333.897	314.061	87.328	99.232	95.375	14.048
2	1168.66	1168.66	0	215.106	215.106	0
3	293.799	236.805	97.204	74.023	75.775	16.424
4	252.703	252.703	29.241	160.766	160.766	8.612
5	363.574	363.574	242.567	112.162	112.162	39.793
6	121.759	121.759	18.71	119.487	119.487	16.797
8	447.741	447.741	0	160.576	160.576	0
9	431.856	431.856	0	188.315	188.315	0
10	471.773	471.773	428.951	94.564	94.564	52.017
11	318.871	158.452	270.968	273.907	158.452	207.728
12	690.614	690.614	0	210.691	210.691	0
13	442.008	513.049	202.859	81.544	67.304	23.898
14	404.015	326.421	270.727	192.309	123.806	176.128
15	287.361	211.628	126.088	88.546	77.409	20.59
16	162.976	162.976	8.802	162.976	162.976	8.802
17	481.399	495.24	84.156	99.082	89.257	28.951
18	1034.929	914.614	206.07	132.259	128.405	18.226
19	707.202	707.202	94.286	115.982	115.982	33.511

Table 3. Integrated cell and nuclei intensities in pLam channel for 10% PMMA surfaces

Image Number	Integrated Cell Intensity Average	Integrated Cell Intensity Median	Standard Deviation Integrated Cell Intensity	Integrated Nuclei Intensity Average	Integrated Nuclei Intensity Average	Standard Deviation Integrated Nuclei Intensity
1	538.943	538.943	0	276.716	276.716	0
2	1339.4	1339.4	33.581	122.636	122.636	37.683
3	658.449	658.449	12.6	156.187	156.187	41.631
4	1128.94	1128.94	547.906	292.98	292.98	108.314
5	1273.52	1227.497	498.056	157.29	174.439	40.572
6	1642.366	1752.328	178.04	187.892	185.401	27.123
7	705.48	705.48	0	293.532	293.532	0
8	1040.347	1040.347	0	356.311	356.311	0
9	525.749	525.749	0	293.532	293.532	0
10	561.499	561.499	458.609	144.057	144.057	108.972
11	4331.438	4331.438	0	600.39	600.39	0
12	316.489	316.489	184.066	160.474	160.474	88.779
13	4356.088	4356.088	0	4166.712	4166.712	0
14	790.528	608.949	262.806	155.678	145.588	45.311
15	281.201	281.201	0	281.201	281.201	0

Table 4. Average of cell and nuclei integrated phosphorylation intensities on each surface as identified by CellProfiler

Surface Type	Average of Integrated Cell Intensities	Average of Integrated Nuclei Intensities
Flat Control Surface	3838.87	261.118
5% PMMA Surface	467.507	143.418
10% PMMA Surface	1372.09	526.028

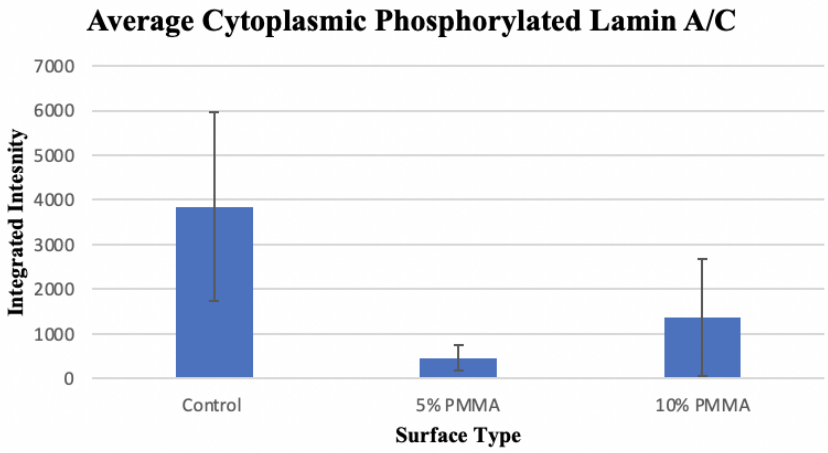

Figure 14. Average cytoplasmic phosphorylated lamin A/C on each surface with error bars that depict the standard deviations

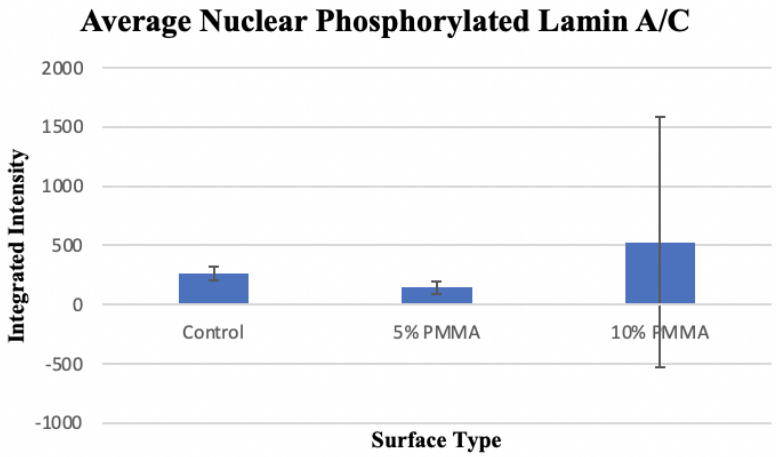

Figure 15. Average nuclear phosphorylated lamin A/C on each surface with error bars that depict the standard deviations

Cell Morphology

Cell and nuclei morphology was found using the measureobjectsizeshape pipeline in CellProfiler. Figure 16 below shows an example of the measureobjectsizeshape pipeline window.

Object	Feature	Mean	Median	STD
Cell	Area	5836.50	5836.50	2278.50
Cell	Perimeter	437.25	437.25	72.15
Cell	MajorAxisLength	159.54	159.54	8.33
Cell	MinorAxisLength	54.06	54.06	21.90
Cell	Eccentricity	0.93	0.93	0.04
Cell	Orientation	-0.78	-0.78	0.15
Cell	Center_X	1015.81	1015.81	124.81
Cell	Center_Y	1275.86	1275.86	450.08
Cell	BoundingBoxArea	15346.50	15346.50	3408.50
Cell	BoundingBoxMinimum_X	946.50	946.50	101.50
Cell	BoundingBoxMaximum_X	1071.00	1071.00	132.00
Cell	BoundingBoxMinimum_Y	1212.50	1212.50	449.50
Cell	BoundingBoxMaximum_Y	1336.50	1336.50	452.50
Cell	FormFactor	0.36	0.36	0.03
Cell	Extent	0.37	0.37	0.07
Cell	Solidity	0.80	0.80	0.01
Cell	Compactness	2.76	2.76	0.22

Figure 16. CellProfiler measureobjectsizeshape window example

This pipeline yields many different terms regarding the shape and size of both the cells and nuclei in each image set. The parameters of interest were area, major axis, minor axis, and form factor. The aspect ratio for each of the image sets was found by dividing the major axis by the minor axis. The closer this value is to 1, the more circle-like in shape. Roundness was also found by the following equation:

$$Roundness = \frac{4 * Area}{\pi * Major\ Axis^2}$$

Equation 1. Roundness Equation

A roundness value closest to 1 also means more circle-like. A value of one refers to a perfect circle. The aspect ratio and roundness values were calculated using the data exported from CellProfiler.

Table 5. Cell morphology data on control surface

Image Number	Area	Major Axis	Minor Axis	Form Factor	Roundness	Aspect Ratio
2	168443	734.19	431.31	0.06	0.397886281	1.702232733
3	100700	601.39	341.63	0.07	0.35451939	1.76035477
4	217838	929.66	398.55	0.04	0.320928494	2.332605696
5	186215.67	919.61	307.05	0.04	0.280370154	2.99498453
6	518021	1296.41	623.41	0.03	0.392451098	2.079546366
7	428570	838.73	480.24	0.33	0.775711696	1.746480926
8	216562.5	626.88	332.85	0.14	0.701677184	1.883370888
9	438331	1162.69	585.96	0.04	0.412854706	1.984248072
10	147440.5	760.85	453.24	0.02	0.32429603	1.678691201
11	122700	784.73	249.45	0.02	0.253703804	3.14584085
12	202152.5	759.66	439.21	0.02	0.44602944	1.729605428
13	117725.5	849.64	275.61	0.03	0.207646	3.082761874
14	274237	908.08	489.84	0.04	0.423448653	1.853829822
15	177405	978.49	383.53	0.06	0.235926106	2.551273694
16	187739.33	967.56	395.97	0.03	0.255342073	2.443518448
17	159727	884.96	337.67	0.03	0.259689255	2.620783605
18	241709	954.17	414.76	0.03	0.338036996	2.300535249
19	243979.33	974.24	436.82	0.05	0.327298525	2.23030081

Table 6. Nuclei morphology data on control surface

Image Number	Area	Major Axis	Minor Axis	Form Factor	Roundness	Aspect Ratio
2	14779	167.58	113.38	0.7	0.67007529	1.47803845
3	7407	74.07	82.04	0.75	1.71901863	0.90285227
4	15287	158.68	128.45	0.63	0.77303794	1.23534449
5	11914	151.75	100.15	0.83	0.65875378	1.51522716
6	22245	210.92	134.74	0.75	0.63667795	1.56538519
7	15293.5	170.3	113.34	0.84	0.67142965	1.50255867
8	12201.5	158.09	100.85	0.54	0.6216234	1.56757561
9	15012	163.03	117.28	0.84	0.71916149	1.39009209
10	12937	153.24	108.47	0.77	0.70147503	1.41274085
11	12079.5	151.78	101.37	0.84	0.66764068	1.49728717
12	13924	158.79	111.67	0.8	0.70313812	1.42195755
13	10088	135.49	95.17	0.86	0.69970264	1.42366292
14	14989.67	163.23	117.24	0.86	0.71633313	1.39227226
15	11333	146.61	98.77	0.85	0.67133707	1.4843576
16	13964	156.75	112.87	0.86	0.72363184	1.38876584
17	12677.25	161.08	102.04	0.71	0.6221065	1.57859663
18	15737.67	173.74	110.99	0.82	0.66384047	1.56536625
19	11866.33	153.72	98.04	0.79	0.63940878	1.56793146

Table 7. Cell morphology data on 5% PMMA surface

Image Number	Area	Major Axis	Minor Axis	Form Factor	Roundness	Aspect Ratio
2	16317.25	278.95	96.45	0.13	0.26700363	2.89217211
3	10395	182.67	72.94	0.63	0.39665503	2.50438717
4	6051.5	150.76	58.14	0.42	0.33901094	2.59305126
5	10248.5	210.71	69.58	0.27	0.29390904	3.02831273
6	10632	292.62	60.4	0.45	0.15809928	4.84470199
7	5081	113.14	57.58	0.71	0.50540528	1.96491837
8	18705	356.73	85.43	0.13	0.18715497	4.1756994
9	15347	267.12	78.84	0.22	0.27386316	3.38812785
10	20400	725.7	57.19	0.41	0.04932179	12.6892813
11	6313.67	130.35	64.5	0.58	0.47313245	2.02093023
12	27332	667.83	86.87	0.04	0.07803016	7.68769426
13	18648	358.35	125.34	0.09	0.18490147	2.85902346
14	13411.6	247.81	94.06	0.22	0.27807751	2.63459494
15	18767.33	275.14	96.24	0.22	0.31565884	2.85889443
16	7720.5	132.23	77.83	0.67	0.56222268	1.69895927
17	27021.33	505.36	119.21	0.09	0.13471871	4.23924167
18	60370.67	800.55	190.28	0.03	0.1199422	4.20722094
19	26437	668.74	111.2	0.06	0.07526975	6.01384892

Table 8. Nuclei morphology data on 5% PMMA surface

Image Number	Area	Major Axis	Minor Axis	Form Factor	Roundness	Aspect Ratio
2	3940	105.92	48.95	0.67	0.44716027	2.16384065
3	10395	182.67	72.94	0.63	0.39665503	2.50438717
4	3189.5	89.45	48.46	0.72	0.50755703	1.84585225
5	6784.5	122.85	70.49	0.71	0.57238791	1.7428004
6	5640.5	103.49	66.14	0.79	0.67056944	1.56471122
7	5081	113.14	57.58	0.71	0.50540528	1.96491837
8	7181	117.77	77.9	0.77	0.65923234	1.51181001
9	9260	148.61	79.45	0.69	0.53387286	1.87048458
10	5040	112.15	55.45	0.7	0.51021698	2.02254283
11	5621.33	131.21	60.43	0.58	0.41574606	2.17127255
12	9578	131.88	92.77	0.72	0.70119673	1.42158025
13	4059.67	106.77	49.37	0.61	0.45343514	2.16264938
14	4895.8	124.29	52.16	0.52	0.40352851	2.38286043
15	3669	96.19	49.45	0.72	0.5049063	1.94519717
16	7720.5	132.23	77.83	0.67	0.56222268	1.69895927
17	5078	105.06	61.93	0.76	0.58578849	1.69643145
18	5999.67	137.39	56.36	0.67	0.40470637	2.43772179
19	4763	118.66	51.55	0.66	0.43071978	2.30184287

Table 9. Cell morphology data on 10% PMMA surface

Image Number	Area	Major Axis	Minor Axis	Form Factor	Roundness	Aspect Ratio
2	16026	252.91	111.3	0.15	0.31901864	2.272327044
3	76474	1112.72	283.46	0.02	0.07864388	3.925492133
4	28801	874.87	57.81	0.05	0.04791191	15.13354091
5	48128.5	545.32	304.21	0.16	0.20607362	1.792577496
6	57651.67	652.71	204	0.06	0.17230357	3.199558824
7	87480.67	765.41	328.1	0.04	0.1901283	2.332855837
8	24321	602.28	67.51	0.08	0.08537043	8.921344986
9	50297	845.14	157.77	0.02	0.08966185	5.356785194
10	16804	479.57	58.94	0.07	0.09303183	8.136579572
11	36679	551.13	150.55	0.06	0.15375608	3.66077715
12	146690	499.12	381.14	0.29	0.74974485	1.309545049
13	5836.5	159.54	54.06	0.36	0.29196866	2.951165372
14	4282	83.73	65.28	0.87	0.7776916	1.282628676
15	67058	1073.17	296.83	0.01	0.07413725	3.615436445
16	11905	165.85	93.69	0.75	0.55108853	1.770199594

Table 10. Nuclei morphology data on 10% PMMA surface

Image Number	Area	Major Axis	Minor Axis	Form Factor	Roundness	Aspect Ratio
2	10273	125.26	105.06	0.69	0.83367236	1.19227108
3	5636.5	116.6	61.05	0.76	0.52788016	1.90990991
4	5276	150.9	44.96	0.57	0.29501849	3.35631673
5	4832	99.06	60.09	0.8	0.6269793	1.64852721
6	6196	130.15	60	0.72	0.46574263	2.16916667
7	7668.33	135.16	73.48	0.76	0.53447495	1.83941208
8	8297	186.96	57	0.42	0.3022363	3.28
9	12673	188.07	86.22	0.61	0.45620844	2.18128045
10	7434	177.64	53.78	0.53	0.29996042	3.30308665
11	11645	147.5	102.07	0.68	0.68151965	1.44508671
12	3213	67.2	61.13	0.89	0.90593097	1.09929658
13	5836	159.53	54.06	0.36	0.29198025	2.95098039
14	4282	83.73	65.28	0.87	0.7776916	1.28262868
15	7917	150.65	67.87	0.64	0.44416599	2.21968469
16	11905	165.85	93.69	0.75	0.55108853	1.77019959

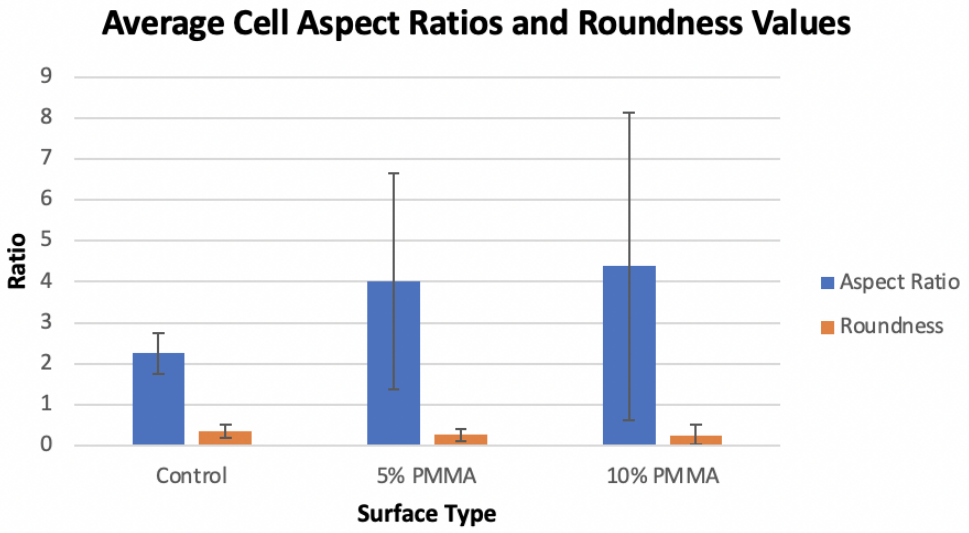

Figure 17. Average cell aspect ratio and roundness values for all surface types

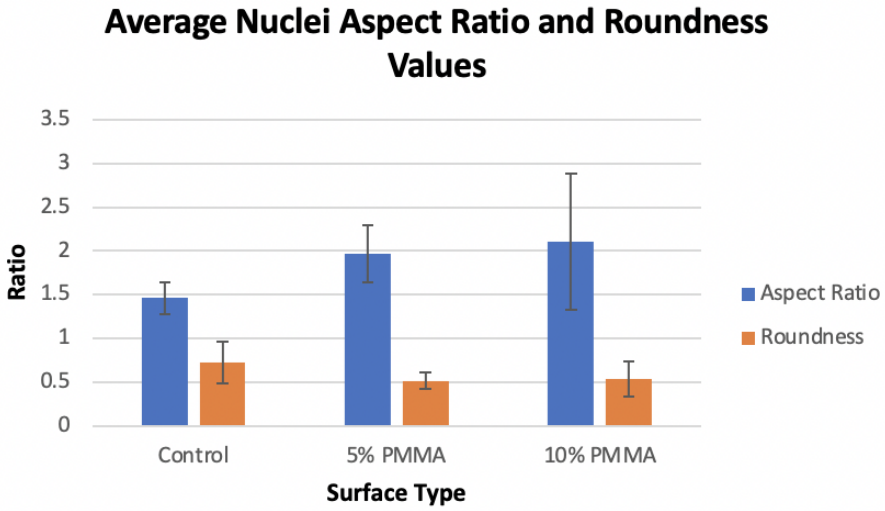

Figure 18. Average nuclei aspect ratio and roundness values for all surface types

Intensity Statistical Testing Results

Table 11. T-test comparing the average cell intensities from the flat control surface and 5% PMMA surface

t-Test: Two-Sample Assuming Unequal Variances		
	Variable 1	*Variable 2*
Mean	3848.8715	467.5076111
Variance	4442626.6	76421.35115
Observations	19	18
Hypothesized Mean Difference	0	
df	19	
t Stat	6.9301291	
P(T<=t) one-tail	6.594E-07	
t Critical one-tail	1.7291328	
P(T<=t) two-tail	1.319E-06	
t Critical two-tail	2.0930241	

Table 12. T-test comparing the average nuclei intensities from the flat control surface and 5% PMMA surface

t-Test: Two-Sample Assuming Unequal Variances		
	Variable 1	*Variable 2*
Mean	261.118632	143.418167
Variance	3057.67656	3086.04822
Observations	19	18
Hypothesized Mean Difference	0	
df	35	
t Stat	6.45598318	
P(T<=t) one-tail	9.7287E-08	
t Critical one-tail	1.68957246	
P(T<=t) two-tail	1.9457E-07	
t Critical two-tail	2.03010793	

Table 13. T-test comparing the average cell intensities from the flat control surface and 10% PMMA surface

t-Test: Two-Sample Assuming Unequal Variances		
	Variable 1	*Variable 2*
Mean	3848.87153	1372.08829
Variance	4442626.56	1722202.98
Observations	19	14
Hypothesized Mean Difference	0	
df	30	
t Stat	4.14622715	
P(T<=t) one-tail	0.00012755	
t Critical one-tail	1.69726089	
P(T<=t) two-tail	0.0002551	
t Critical two-tail	2.04227246	

Table 14. T-test comparing the average nuclei intensities from the flat control surface and 10% PMMA surface

t-Test: Two-Sample Assuming Unequal Variances		
	Variable 1	*Variable 2*
Mean	261.118632	526.027643
Variance	3057.67656	1113845.54
Observations	19	14
Hypothesized Mean Difference	0	
df	13	
t Stat	-0.9382303	
P(T<=t) one-tail	0.18261569	
t Critical one-tail	1.7709334	
P(T<=t) two-tail	0.36523137	
t Critical two-tail	2.16036866	

Table 15. T-test comparing the average cell intensities from the 5% PMMA surface and 10% PMMA surface

t-Test: Two-Sample Assuming Unequal Variances		
	Variable 1	*Variable 2*
Mean	467.50761	1372.08829
Variance	76421.351	1722202.98
Observations	18	14
Hypothesized Mean Difference	0	
df	14	
t Stat	-2.535719	
P(T<=t) one-tail	0.0118831	
t Critical one-tail	1.7613101	
P(T<=t) two-tail	0.0237663	
t Critical two-tail	2.1447867	

Table 16. T-test comparing the average nuclei intensities from the 5% PMMA surface and 10% PMMA surface

t-Test: Two-Sample Assuming Unequal Variances		
	Variable 1	*Variable 2*
Mean	143.4181667	526.0276429
Variance	3086.048217	1113845.539
Observations	18	14
Hypothesized Mean Difference	0	
df	13	
t Stat	-1.355001641	
P(T<=t) one-tail	0.099247917	
t Critical one-tail	1.770933396	
P(T<=t) two-tail	0.198495835	
t Critical two-tail	2.160368656	

Morphology Statistical Testing Results

Table 17. T-test comparing the average of nuclei aspect ratios from the control surface and 5% PMMA surface

t-Test: Two-Sample Assuming Unequal Variances		
	Variable 1	*Variable 2*
Mean	1.4620072	1.96721459
Variance	0.0325787	0.10609219
Observations	20	18
Hypothesized Mean Difference	0	
df	26	
t Stat	-5.8247302	
P(T<=t) one-tail	1.937E-06	
t Critical one-tail	1.7056179	
P(T<=t) two-tail	3.874E-06	
t Critical two-tail	2.0555294	

Table 18. T-test comparing the average of nuclei aspect ratios from the control surface and 10% PMMA surface

t-Test: Two-Sample Assuming Unequal Variances		
	Variable 1	*Variable 2*
Mean	1.46200716	2.10985649
Variance	0.03257867	0.60754266
Observations	20	15
Hypothesized Mean Difference	0	
df	15	
t Stat	-3.1562335	
P(T<=t) one-tail	0.00326133	
t Critical one-tail	1.75305036	
P(T<=t) two-tail	0.00652266	
t Critical two-tail	2.13144955	

Table 19. T-test comparing the average of nuclei aspect ratios from the 5% PMMA surface and 10% PMMA surface

t-Test: Two-Sample Assuming Unequal Variances		
	Variable 1	*Variable 2*
Mean	1.967214592	2.10985649
Variance	0.106092189	0.60754266
Observations	18	15
Hypothesized Mean Difference	0	
df	18	
t Stat	-0.662220855	
P(T<=t) one-tail	0.258109744	
t Critical one-tail	1.734063607	
P(T<=t) two-tail	0.516219488	
t Critical two-tail	2.10092204	

Table 20. T-test comparing average cell aspect ratios of the control and 5% PMMA surfaces

t-Test: Two-Sample Assuming Unequal Variances		
	Variable 1	*Variable 2*
Mean	2.251469548	4.01672557
Variance	0.251548865	6.97537483
Observations	20	18
Hypothesized Mean Difference	0	
df	18	
t Stat	-2.790772069	
P(T<=t) one-tail	0.00603651	
t Critical one-tail	1.734063607	
P(T<=t) two-tail	0.012073019	
t Critical two-tail	2.10092204	

Table 21. T-test comparing the cell aspect ratios of the control and 10% PMMA surfaces

t-Test: Two-Sample Assuming Unequal Variances		
	Variable 1	*Variable 2*
Mean	2.251469548	4.37738762
Variance	0.251548865	14.0880057
Observations	20	15
Hypothesized Mean Difference	0	
df	14	
t Stat	-2.179107887	
P(T<=t) one-tail	0.023449553	
t Critical one-tail	1.761310136	
P(T<=t) two-tail	0.046899107	
t Critical two-tail	2.144786688	

Table 22. T-test comparing average cell aspect ratios of 5% PMMA and 10% PMMA surfaces

t-Test: Two-Sample Assuming Unequal Variances		
	Variable 1	*Variable 2*
Mean	4.01672557	4.37738762
Variance	6.97537483	14.0880057
Observations	18	15
Hypothesized Mean Difference	0	
df	25	
t Stat	-0.3131199	
P(T<=t) one-tail	0.37839348	
t Critical one-tail	1.70814076	
P(T<=t) two-tail	0.75678696	
t Critical two-tail	2.05953855	

Chapter 4

Discussion

The hypothesis of this research was that the difference between the average integrated cell and nuclei intensities between the three surfaces, the control and two PMMA surfaces, would be statistically significant. This was hypothesized because as seen in previous nuclear lamina studies, different characteristics of stem cell engineering scaffold surfaces impact the way a cell responds to the surface itself. These interactions are imperative for better understanding what is occurring on a molecular level when stem cells are applied to different surface types. The t-tests above were conducted between each of the different surfaces and the two different intensities studied for a total of six unique t-tests: average nuclei intensity between control and 5% PMMA surface, average nuclei intensity between control and 5% PMMA surface, average cell intensity between control and 10% PMMA surface, average nuclei intensity between control and 10% PMMA surface, average cell intensity between 5% PMMA and 10% PMMA surface, and average nuclei intensity between 5% PMMA and 10% PMMA surfaces. Each of the tests were conducted with a confidence level of 0.05 on Microsoft Excel. Each test yielded a p value (two tailed) that could be compared to this confidence level in order to determine statistical significance.

Control Surface vs 5% PMMA Surface Intensities Statistical Discussion

When comparing the average cell intensity between the control surface and the 5% PMMA surface with a t-test, the two-tailed p-value was found to be $6.59*10^{-7}$. This value is much less than the confidence level of 0.05. This means that the difference between the average cell intensities found on the control plate vs found on the 5% PMMA plate is statistically significant. A t-test was then performed between the average nuclei integrated intensities between the control and 5% PMMA surfaces as well. This resulted in a two-tailed p value of $1.95*10^{-7}$. This is also much less than the confidence level of 0.05.

This means there is a statistically significant difference between the average nuclei intensities of the 5% PMMA and the control plates that is not due to random chance.

Both of these t-tests support the initial hypothesis that there would be a statistical significance between the cell and nuclei intensities of phosphorylated lamina on different surface types. This means that the difference between the average intensities on the control surface and 5% PMMA surface are not due to random chance; the surface properties influenced this difference of intensity averages. There are many potential explanations of these results, but none can be confirmed without further testing. The surface area of a nanofiber scaffold is much larger than the bottom of a sterilized plate. Cells may be able to better anchor themselves to the surface of a fiber because they are able to wrap around the circular cross section using filipodia and cellular adhesion proteins. Phosphorylated lamin have also been studied with respect to cellular division and migration. The cells present on the control surface may have more migratory abilities than those adhered to the fibrous scaffolds and thus may have an increased concentration of phosphorylated lamina. The cells present on the PMMA surface may be adhered and primarily stretch while on the fibers rather than migrate in any way.

Control Surface vs 10% PMMA Surface Intensities Statistical Discussion

The two-tailed p value that resulted in the t-test performed to compare the control surface and the 10% PMMA surface integrated average cell intensities was found to be 0.0002551. This value was much less than the confidence level of 0.05. This means that the difference between the average cell intensities of the two surfaces is statistically significant. The p-value from the t-test performed to compare the average nuclei intensities was found to be 0.36523. This value is larger than the 0.05 confidence level. This means that the difference between the average integrated nuclei intensity for the control surface and 10% PMMA surface is not statistically significant.

These findings indicate that phosphorylated cytoplasmic lamin A/C was more prevalent on the control surface than on the 10% PMMA surface and that this difference is not due to random chance. High levels of cytoplasmic phosphorylated lamin A/C may indicate cells undergoing division because as the nuclear envelope breaks down, the phosphorylated lamin remain within the cytoplasm as they prepare to form spindles for chromosomal separation. This may also mean cells found on the fibrous surface of 10% PMMA may have been more adhered to their surface. The difference between the average nuclei intensities was not statistically significant, which could be due to error in data collection or quantification. Error is likely because previous studies have seen that nuclear lamina likely phosphorylate in response to different surfaces. This could also mean that the cells interact with both surfaces in a similar manner but based on previous research of the importance of nanofiber interactions with stem cells this seems unlikely. It could also potentially indicate that phosphorylated lamin localized in the cytoplasm are more influential on studies of lamin and environmental sensing. Studies can be continued on the localization of phosphorylated lamin to better understand what exactly is happening and why it is happening.

5% PMMA Surface vs 10% PMMA Surface Intensities Statistical Discussion

The two-tailed p value that resulted in the t-test performed to compare the 5% PMMA surface and the 10% PMMA surface integrated average cell intensities was found to be 0.0237663. This value is less than the confidence level of 0.05, which means that average cell intensities between the PMMA surfaces are statistically significant. Statistical significance means that these average values are not due to random chance. The p value from the t-test

performed to compare the average integrated nuclei intensities between the two PMMA surfaces was found to be 0.198. This value is larger than the 0.05 confidence level, which means the difference between the mean nuclei intensities is not statistically significant.

These findings indicate that phosphorylated cytoplasmic lamin A/C was more prevalent in the 5% PMMA surface than in the 10% PMMA surface and that this difference is not due to random chance. As discussed above, there may be many reasons for this statistical significance, but one could possibly lie in the number of dividing cells on either surface. Cytoplasmic phosphorylated lamin A/C could indicate the stages of cellular division that follow nuclear membrane breakdown or a more mobile cell. The difference between the average nuclei intensities on the 5% and 10% PMMA surface was not statistically significant. This could be simply due to error because the difference between the average intensities of cytoplasmic phosphorylated lamina was significant, but it could also be due to another phenomenon not previously studied. Based on the results of this study, more research is needed in the field of nuclear lamina phosphorylation and localization.

Cell and Nuclei Morphology

A previous study conducted about nuclear lamina responding to ECM elasticity found that a higher lamin A:B ratio results in nuclei that are oblong, oval shaped [21]. A low lamin A:B ratio was found to result in nuclei that are rounder, more circular in nature [21]. Figure 10 shows the identification of nuclei and cells on a control surface. The nuclei highlighted from CellProfiler appear rounded and circular in nature. According to Swift and Discher, this would mean the phosphorylated lamin present on control surfaces likely possess a low lamin A:B ratio.

Figures 11 and 12 depict identified cells and nuclei that are much more oblong in shape when compared to those present on the control surface. This may likely mean that the lamin present have a high A:B type ratio. This ratio is important because it has been determined that a very small or very large level of lamin A may indicate low cell migration [21]. Lamina A is known to promote stability in a cell's overall structure so a high amount of this lamin type can inhibit migration by increasing stability in the cell overall [21]. However, this does not mean that the cells are not spreading at all. Stiffer cells may adhere to the fibers and spread out over a larger surface area. Cellular spreading allows cells to adhere to the surface, while also interacting with neighboring spreading cells. This facilitates tissue formation over time. The PMMA surfaces, as shown by the presence of oblong nuclei, may indicate slower cell migration, while also indicating cellular surface adhesion. This could be due to many reasons such as a faster overall adherence to the PMMA surfaces or the stage of the cell cycle that the cell was currently in when it was imaged. This phenomenon could also potentially explain some of the above statistical results. Concrete conclusions cannot be drawn just from the data within this study, but this phenomenon of lamin ratio changing based on surface stiffness may play a role in better understanding the changing stem cell morphologies in regenerative medicine.

T-tests were also performed between the nuclei aspect ratios to determine if the shapes seen were significantly different. The above conclusions were further validated from the t-test results on nuclei aspect ratio. The p-value when comparing the aspect ratios between the 5% PMMA and 10% PMMA surfaces was found to be 0.5162, which is much larger than the confidence level of 0.05. This means that the means are not statistically significant, which follows what was expected. The p-value from the t-test between the control and 5% PMMA surface was found to be $3.874*10^{-6}$. This value is much smaller than the confidence level of 0.05,

which means the difference between the average nuclei of the control and 5% PMMA surfaces is statistically significant. The p-value for the t-test conducted between the control surface and the 10% PMMA surface was found to be 0.00652. This also indicates that the difference between the nuclei aspect ratio of the control and 10% PMMA surfaces is statistically significant as well. These statistical tests indicated that the nanofiber nucleus shape was affected by the PMMA surface.

T-tests were also performed between the average cell aspect ratios as well. The p value between the control surface and 5% PMMA surface was 0.012. This value is less than the confidence level of 0.05, which means there is a statistical significance between the average cell aspect ratios found on the control and 5% PMMA surface. The p value between the control surface and 10% PMMA surface was found to be 0.046. This is also less than 0.05 and thus there is a statistical significance between the cell aspect ratios found on these two surfaces. The t-test comparing the 5% PMMA and 10% PMMA surfaces was found to be 0.0756. This is much larger than 0.05 and thus there is not a statistical significance between the cell aspect ratios found between the PMMA surfaces.

This all means that nanofiber surfaces likely cause a change in cellular shape when compared to traditional flat plates. This is expected based on previous studies because cells on fibrous surfaces tend to adhere, then wrap around, and stretch on the surface to fill the voids of the porous structures.

Chapter 5

Conclusion

Limitations

The statistical testing yielded that there was significance between the average values of integrated cellular phosphorylated lamin A/C when comparing all three of the surfaces to one another. It also indicated statistical significance between the average nuclei intensities of phosphorylated lamin A/C of the control and 5% PMMA surfaces. These t-tests also determined that there was not a statistical significance between the nuclei averages between the control and 10% PMMA surface as well as between the 5% and 10% PMMA surfaces. A possible explanation for these results could be not a large enough sample size. Larger sample sizes can improve statistical significance if there is an error in any of the inputted data. This could include obtaining 30 images rather than slightly under 20 of the live cells on the different surface types. Error is also likely either in data collection or data quantification because there is statistical significance between many of the averages compared, but not all of the averages compared, which does not follow what should be expected. The standard deviation of the average nuclei intensity on 10% PMMA is larger than the overall average. This means there must be error in data collection and/or quantification. There is one outlier within table in the 13th set of images. This nuclei average is an order of magnitude higher than the other recorded values. Data quantification was done twice, which means this discrepancy must lie in CellProfiler use or the image collected.

This study was also limited in the surfaces studied. A more complex study could include more surfaces of varying diameters and/or surfaces of a different biocompatible polymer other

than PMMA. These surfaces of varying stiffness can change nuclear lamina composition and overall cell morphology. This will allow further research into the mechano-sensing capabilities of nuclear lamina too as discussed above.

Future Impact

Nuclear lamina research can open many doors in the future of biological and clinical research. The mechano-sensing capabilities of the lamina can be further researched on surfaces of varying stiffness. This will allow researchers to gather a plethora of research into the most ideal scaffold for individual stem cell engineering studies and applications. Because lamina either inhibit or promote cell migration, they also can be studied in terms of cancer metastasis. The ratio between lamina types can be studied to understand how cells, specifically cancer cells, migrate throughout the body [8]. This research can focus on how to induce the ideal ratio of lamina types to prevent migration of abnormal cells to slow or completely inhibit cancer spreading [8]. If cancer cell metastasis can be blocked in any way, treatment options can focus on localized doses of radiation. Cells found with high levels of lamin A are overall stiffer and cannot migrate between tissues as a result of their increased rigidity [8].

The field of regenerative medicine becomes more innovative as biomedical research and technology continues to evolve. Stem cell engineering, although only one aspect of regenerative medicine, is at the forefront of current bioengineering research. The overall steps on culturing cells, applying cells to surfaces, and studying the cells once they proliferate as desired can be modified for each researcher's end goal. Small aspects within the overall stem cell engineering outline can be modified to better understand the impact that different changes have on tissue

growth. The nuclear lamina plays a huge role in the way stem cells respond to the surfaces they grow on. Between their mechano-sensing abilities and their impact on cellular motility, understanding the nuclear lamina will allow extensive improvements in the field of regenerative medicine for years to come.

Appendix A: CellProfiler Identification of Phosphorylated Lamin in Nuclei and Cytoplasm

CellProfiler Images of Live Cells: Control Surface Cells

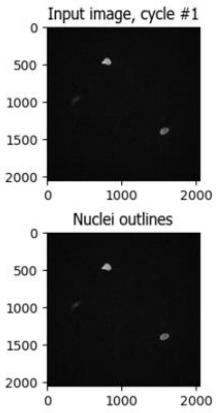

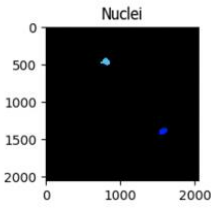

# of accepted objects	2
10th pctile diameter	100.6 pixels
Median diameter	104.3 pixels
90th pctile diameter	104.3 pixels
Area covered by objects	0.4 %
Thresholding filter size	1.0
Threshold	0.0113

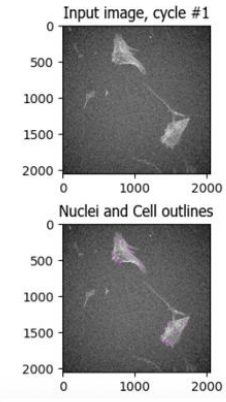

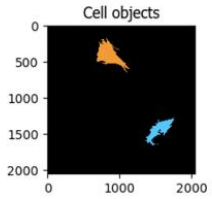

Threshold	0.0188
10th pctile diameter	263.5 pixels
Median diameter	321.0 pixels
90th pctile diameter	321.0 pixels
Thresholding filter size	0.0
Area covered by objects	3.2 %

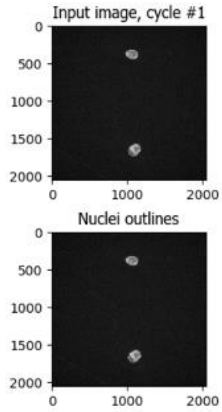

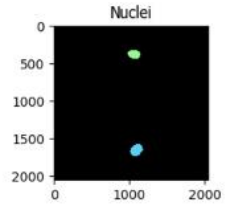

# of accepted objects	2
10th pctile diameter	141.3 pixels
Median diameter	161.3 pixels
90th pctile diameter	161.3 pixels
Area covered by objects	0.9 %
Thresholding filter size	1.0
Threshold	0.00886

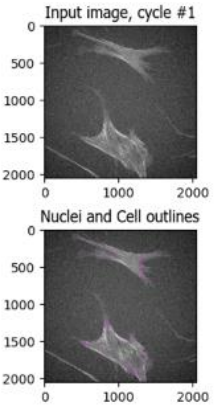

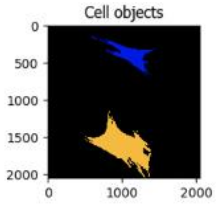

Threshold	0.019
10th pctile diameter	354.9 pixels
Median diameter	577.7 pixels
90th pctile diameter	577.7 pixels
Thresholding filter size	0.0
Area covered by objects	8.6 %

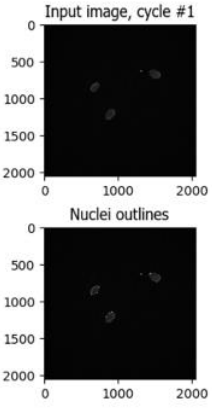

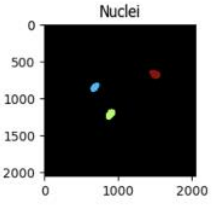

# of accepted objects	3
10th pctile diameter	117.9 pixels
Median diameter	131.5 pixels
90th pctile diameter	134.4 pixels
Area covered by objects	0.9 %
Thresholding filter size	1.0
Threshold	0.00972

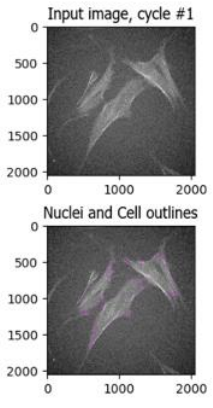

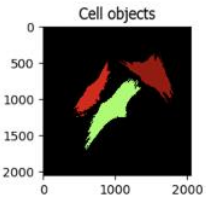

Threshold	0.0173
10th pctile diameter	384.1 pixels
Median diameter	481.4 pixels
90th pctile diameter	526.3 pixels
Thresholding filter size	0.0
Area covered by objects	12.3 %

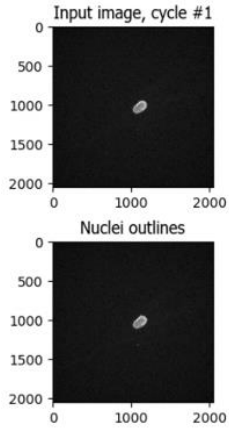

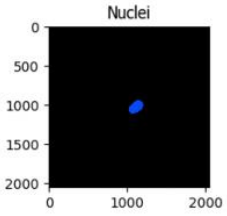

# of accepted objects	1
10th pctile diameter	168.3 pixels
Median diameter	168.3 pixels
90th pctile diameter	168.3 pixels
Area covered by objects	0.5 %
Thresholding filter size	1.0
Threshold	0.00757

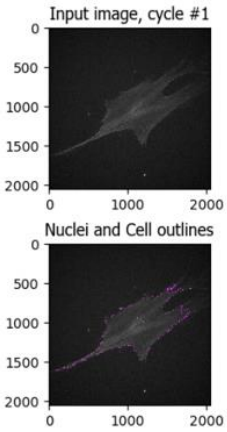

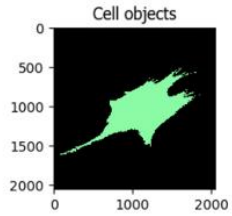

Threshold	0.0177
10th pctile diameter	812.1 pixels
Median diameter	812.1 pixels
90th pctile diameter	812.1 pixels
Thresholding filter size	0.0
Area covered by objects	12.4 %

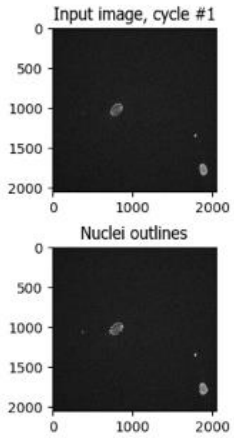

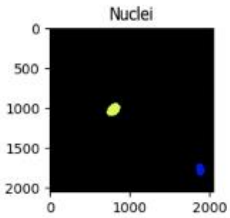

# of accepted objects	2
10th pctile diameter	130.3 pixels
Median diameter	161.0 pixels
90th pctile diameter	161.0 pixels
Area covered by objects	0.8 %
Thresholding filter size	1.0
Threshold	0.00502

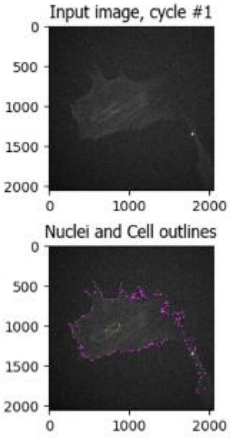

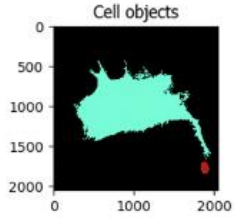

Threshold	0.0112
10th pctile diameter	130.8 pixels
Median diameter	1037.1 pixels
90th pctile diameter	1037.1 pixels
Thresholding filter size	0.0
Area covered by objects	20.5 %

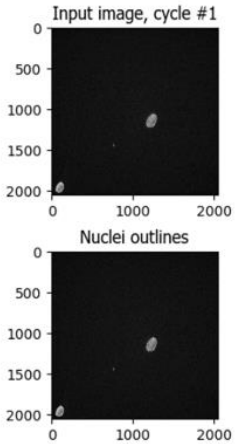

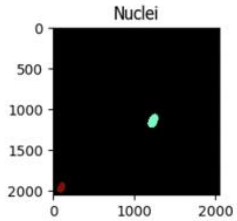

# of accepted objects	2
10th pctile diameter	113.1 pixels
Median diameter	145.2 pixels
90th pctile diameter	145.2 pixels
Area covered by objects	0.6 %
Thresholding filter size	1.0
Threshold	0.0112

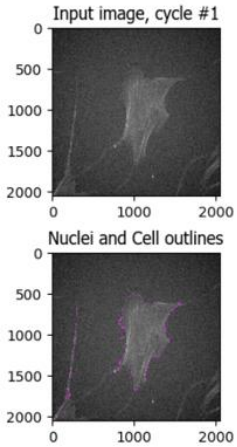

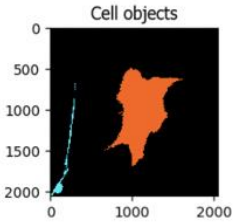

Threshold	0.0158
10th pctile diameter	203.3 pixels
Median diameter	778.0 pixels
90th pctile diameter	778.0 pixels
Thresholding filter size	0.0
Area covered by objects	12.1 %

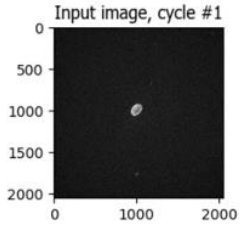

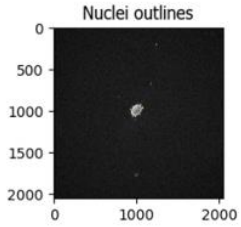

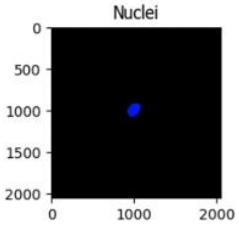

# of accepted objects	1
10th pctile diameter	156.9 pixels
Median diameter	156.9 pixels
90th pctile diameter	156.9 pixels
Area covered by objects	0.5 %
Thresholding filter size	1.0
Threshold	0.00584

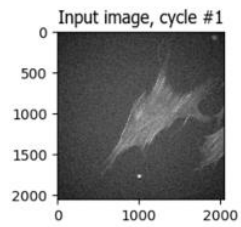

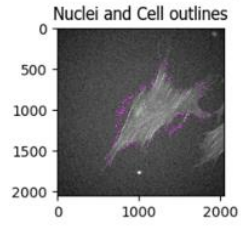

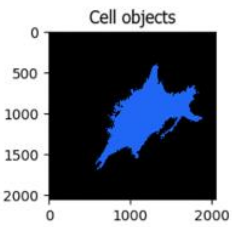

Threshold	0.016
10th pctile diameter	869.5 pixels
Median diameter	869.5 pixels
90th pctile diameter	869.5 pixels
Thresholding filter size	0.0
Area covered by objects	14.2 %

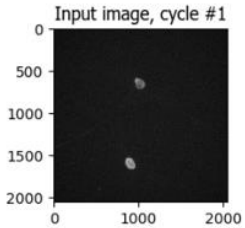

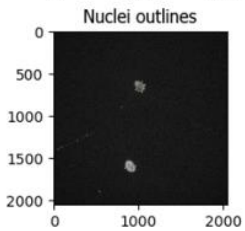

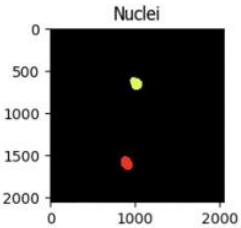

# of accepted objects	2
10th pctile diameter	145.8 pixels
Median diameter	151.8 pixels
90th pctile diameter	151.8 pixels
Area covered by objects	0.8 %
Thresholding filter size	1.0
Threshold	0.00604

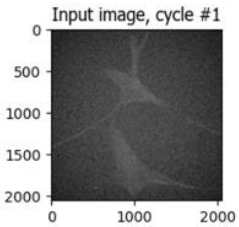

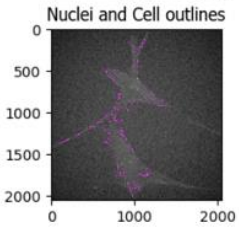

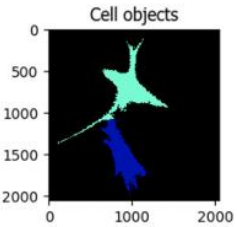

Threshold	0.0155
10th pctile diameter	475.4 pixels
Median diameter	519.0 pixels
90th pctile diameter	519.0 pixels
Thresholding filter size	0.0
Area covered by objects	9.3 %

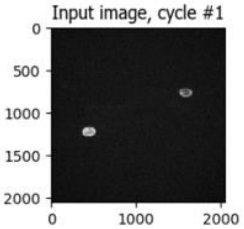

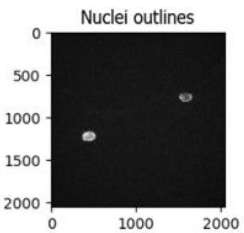

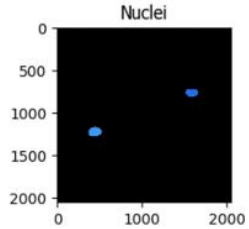

# of accepted objects	2
10th pctile diameter	118.8 pixels
Median diameter	132.1 pixels
90th pctile diameter	132.1 pixels
Area covered by objects	0.6 %
Thresholding filter size	1.0
Threshold	0.011

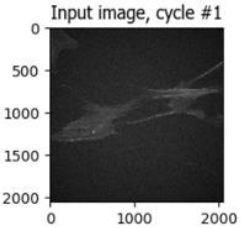

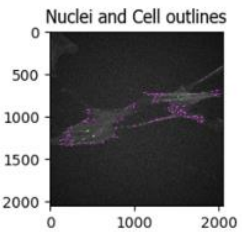

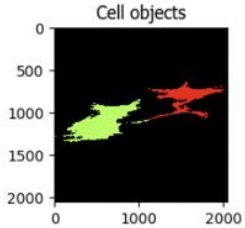

Threshold	0.0176
10th pctile diameter	378.2 pixels
Median diameter	509.9 pixels
90th pctile diameter	509.9 pixels
Thresholding filter size	0.0
Area covered by objects	7.5 %

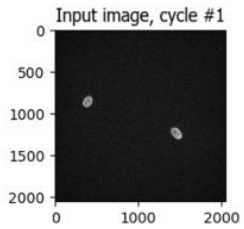

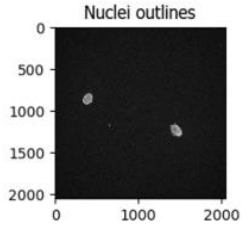

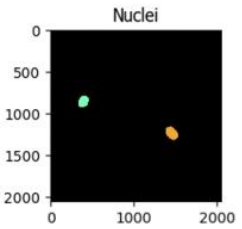

# of accepted objects	2
10th pctile diameter	135.6 pixels
Median diameter	151.4 pixels
90th pctile diameter	151.4 pixels
Area covered by objects	0.8 %
Thresholding filter size	1.0
Threshold	0.00604

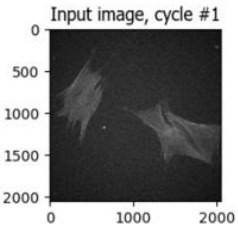

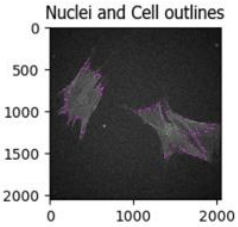

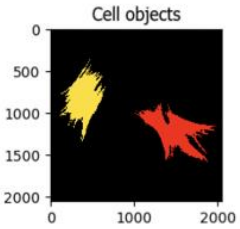

Threshold	0.0183
10th pctile diameter	508.6 pixels
Median diameter	552.7 pixels
90th pctile diameter	552.7 pixels
Thresholding filter size	0.0
Area covered by objects	10.6 %

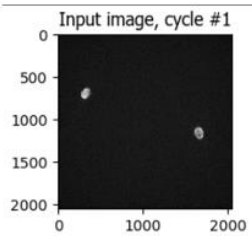

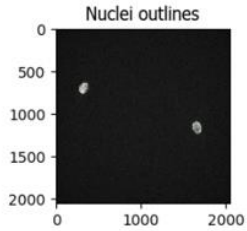

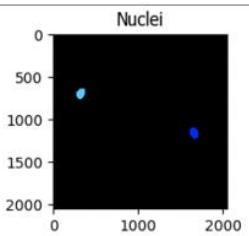

# of accepted objects	2
10th pctile diameter	112.9 pixels
Median diameter	117.6 pixels
90th pctile diameter	117.6 pixels
Area covered by objects	0.5 %
Thresholding filter size	1.0
Threshold	0.0114

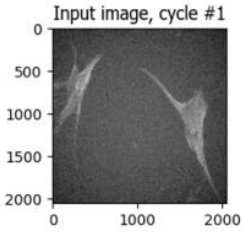

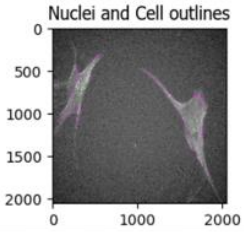

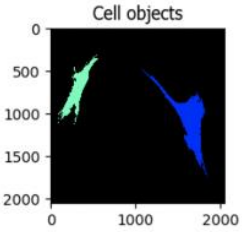

Threshold	0.0181
10th pctile diameter	338.1 pixels
Median diameter	461.9 pixels
90th pctile diameter	461.9 pixels
Thresholding filter size	0.0
Area covered by objects	6.1 %

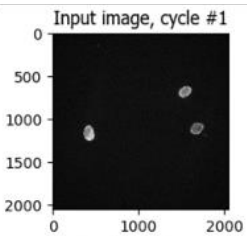

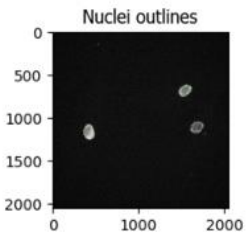

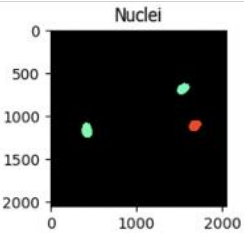

# of accepted objects	3
10th pctile diameter	134.0 pixels
Median diameter	138.8 pixels
90th pctile diameter	147.0 pixels
Area covered by objects	1.1 %
Thresholding filter size	1.0
Threshold	0.0118

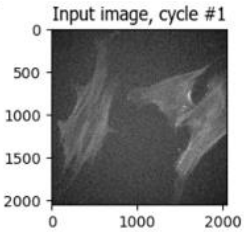

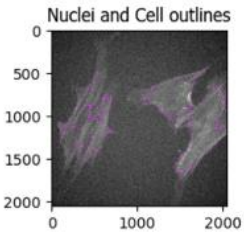

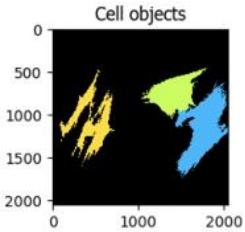

Threshold	0.0179
10th pctile diameter	490.7 pixels
Median diameter	500.1 pixels
90th pctile diameter	622.2 pixels
Thresholding filter size	0.0
Area covered by objects	16.4 %

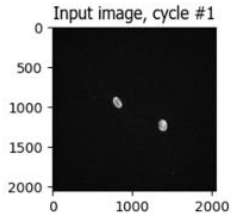

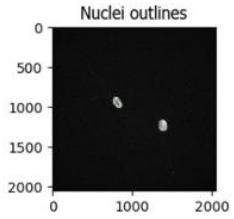

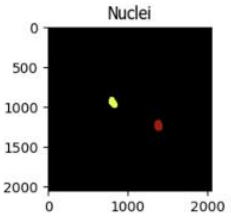

# of accepted objects	2
10th pctile diameter	117.4 pixels
Median diameter	125.6 pixels
90th pctile diameter	125.6 pixels
Area covered by objects	0.6 %
Thresholding filter size	1.0
Threshold	0.0146

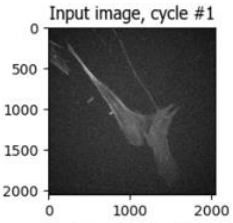

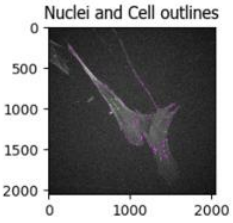

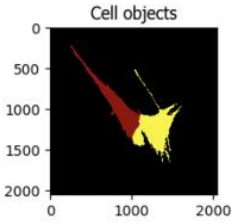

Threshold	0.0182
10th pctile diameter	433.6 pixels
Median diameter	479.7 pixels
90th pctile diameter	479.7 pixels
Thresholding filter size	0.0
Area covered by objects	7.8 %

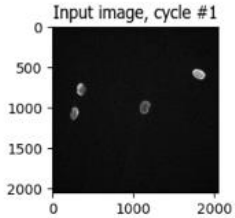

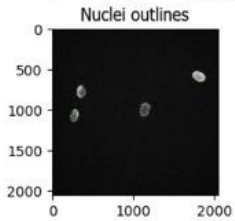

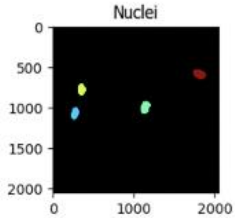

# of accepted objects	4
10th pctile diameter	121.5 pixels
Median diameter	138.9 pixels
90th pctile diameter	138.9 pixels
Area covered by objects	1.3 %
Thresholding filter size	1.0
Threshold	0.0119

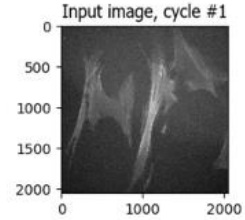

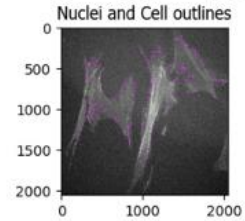

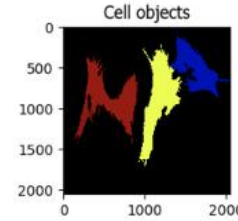

Threshold	0.0195
10th pctile diameter	230.3 pixels
Median diameter	562.2 pixels
90th pctile diameter	612.2 pixels
Thresholding filter size	0.0
Area covered by objects	18.6 %

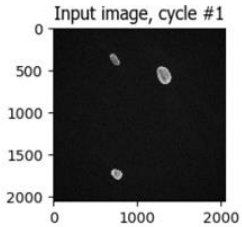

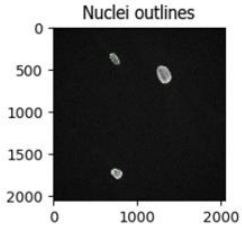

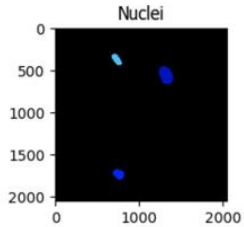

# of accepted objects	3
10th pctile diameter	115.5 pixels
Median diameter	123.5 pixels
90th pctile diameter	186.7 pixels
Area covered by objects	1.2 %
Thresholding filter size	1.0
Threshold	0.0101

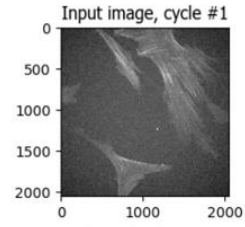

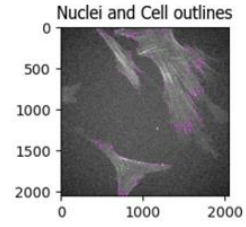

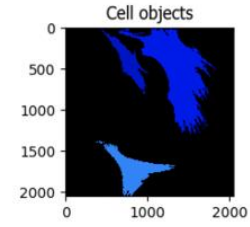

Threshold	0.017
10th pctile diameter	367.6 pixels
Median diameter	465.9 pixels
90th pctile diameter	817.2 pixels
Thresholding filter size	0.0
Area covered by objects	19.1 %

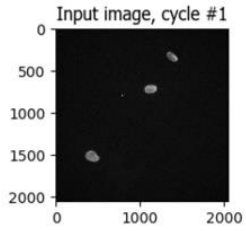

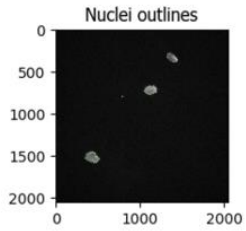

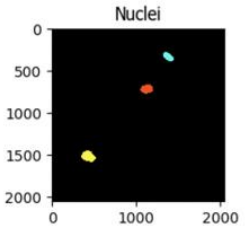

# of accepted objects	3
10th pctile diameter	109.6 pixels
Median diameter	127.4 pixels
90th pctile diameter	142.9 pixels
Area covered by objects	0.9 %
Thresholding filter size	1.0
Threshold	0.01

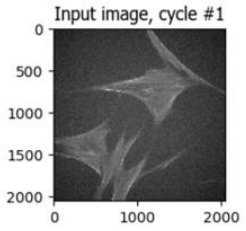

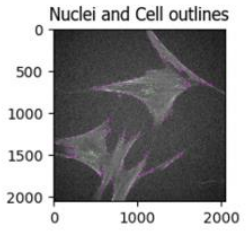

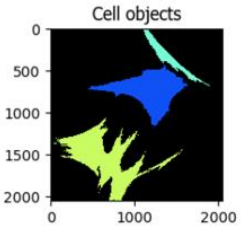

Threshold	0.0171
10th pctile diameter	299.7 pixels
Median diameter	633.1 pixels
90th pctile diameter	708.1 pixels
Thresholding filter size	0.0
Area covered by objects	18.6 %

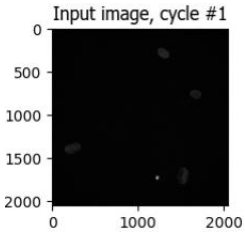

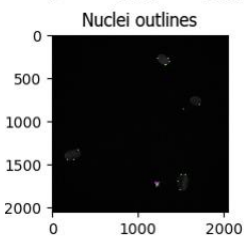

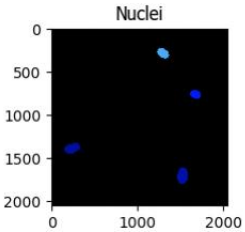

# of accepted objects	4
10th pctile diameter	112.9 pixels
Median diameter	149.9 pixels
90th pctile diameter	158.4 pixels
Area covered by objects	1.4 %
Thresholding filter size	1.0
Threshold	0.00986

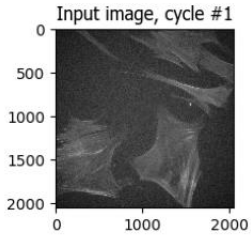

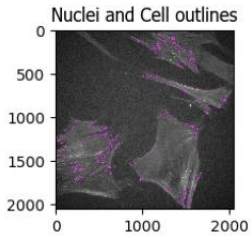

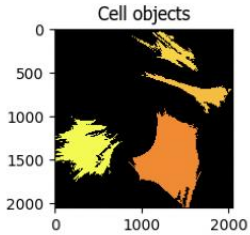

Threshold	0.0176
10th pctile diameter	337.7 pixels
Median diameter	592.0 pixels
90th pctile diameter	776.5 pixels
Thresholding filter size	0.0
Area covered by objects	22.4 %

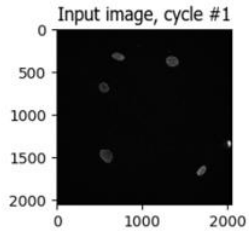

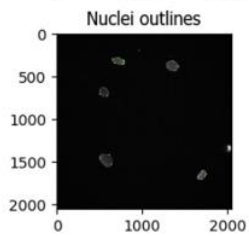

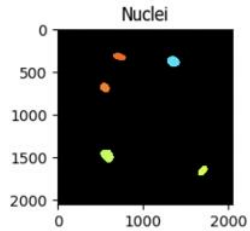

# of accepted objects	5
10th pctile diameter	106.5 pixels
Median diameter	112.8 pixels
90th pctile diameter	150.3 pixels
Area covered by objects	1.4 %
Thresholding filter size	1.0
Threshold	0.0114

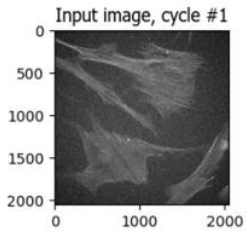

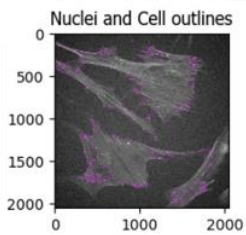

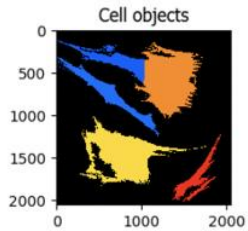

Threshold	0.0172
10th pctile diameter	330.4 pixels
Median diameter	419.3 pixels
90th pctile diameter	707.4 pixels
Thresholding filter size	0.0
Area covered by objects	26.6 %

CellProfiler Images of Live Cells: 5% PMMA Surface

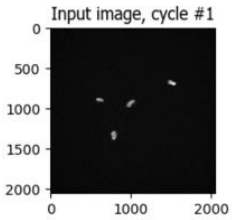

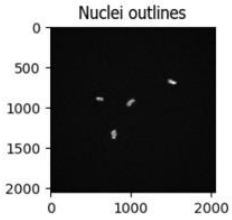

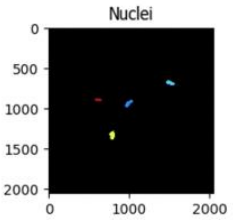

# of accepted objects	4
10th pctile diameter	64.4 pixels
Median diameter	80.4 pixels
90th pctile diameter	85.8 pixels
Area covered by objects	0.4 %
Thresholding filter size	1.0
Threshold	0.0121

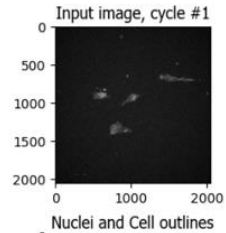

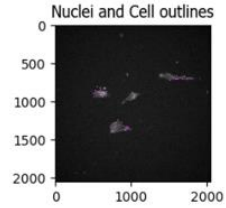

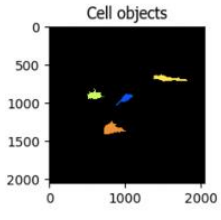

Threshold	0.0205
10th pctile diameter	125.6 pixels
Median diameter	157.9 pixels
90th pctile diameter	179.2 pixels
Thresholding filter size	0.0
Area covered by objects	1.7 %

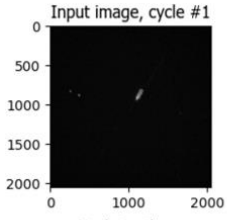

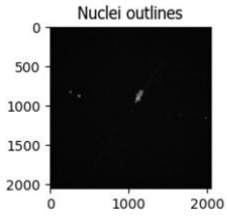

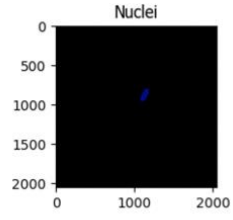

# of accepted objects	1
10th pctile diameter	118.9 pixels
Median diameter	118.9 pixels
90th pctile diameter	118.9 pixels
Area covered by objects	0.3 %
Thresholding filter size	1.0
Threshold	0.00737

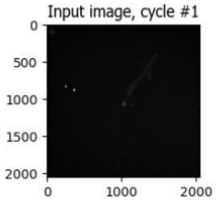

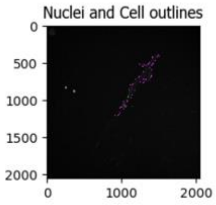

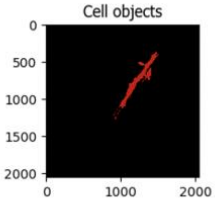

Threshold	0.0195
10th pctile diameter	291.9 pixels
Median diameter	291.9 pixels
90th pctile diameter	291.9 pixels
Thresholding filter size	0.0
Area covered by objects	1.6 %

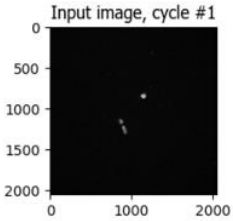

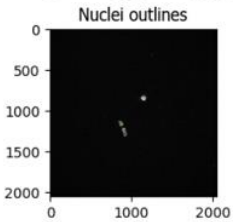

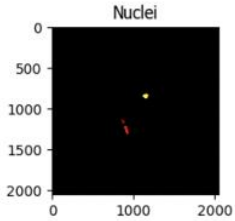

# of accepted objects	3
10th pctile diameter	48.7 pixels
Median diameter	60.5 pixels
90th pctile diameter	66.8 pixels
Area covered by objects	0.2 %
Thresholding filter size	1.0
Threshold	0.0205

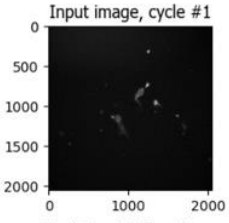

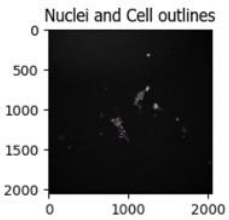

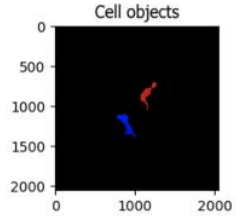

Threshold	0.0198
10th pctile diameter	113.7 pixels
Median diameter	126.6 pixels
90th pctile diameter	163.6 pixels
Thresholding filter size	0.0
Area covered by objects	1.0 %

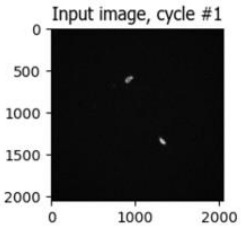

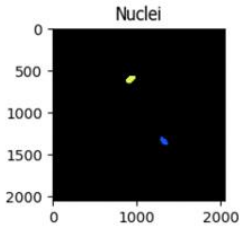

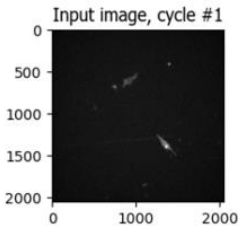

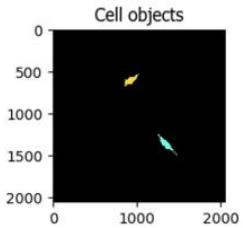

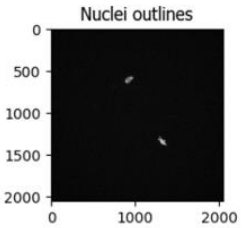

# of accepted objects	2
10th pctile diameter	86.9 pixels
Median diameter	98.6 pixels
90th pctile diameter	98.6 pixels
Area covered by objects	0.3 %
Thresholding filter size	1.0
Threshold	0.00732

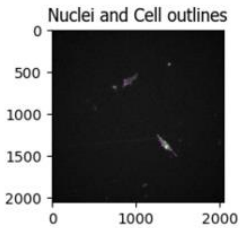

Threshold	0.0247
10th pctile diameter	116.1 pixels
Median diameter	123.1 pixels
90th pctile diameter	123.1 pixels
Thresholding filter size	0.0
Area covered by objects	0.5 %

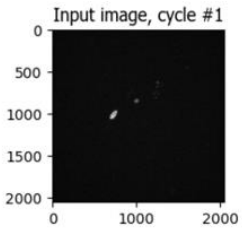

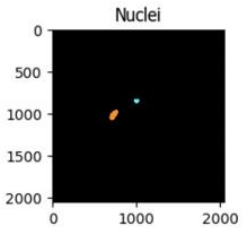

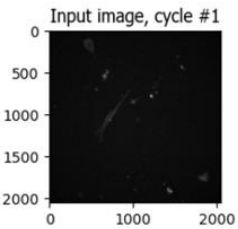

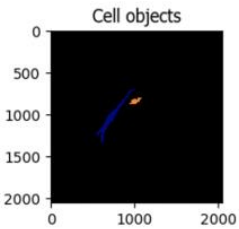

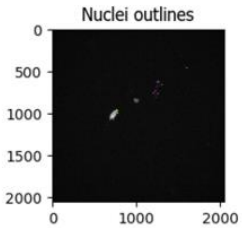

# of accepted objects	2
10th pctile diameter	61.4 pixels
Median diameter	102.9 pixels
90th pctile diameter	102.9 pixels
Area covered by objects	0.3 %
Thresholding filter size	1.0
Threshold	0.00732

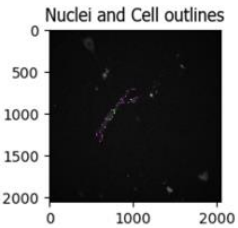

Threshold	0.0184
10th pctile diameter	86.8 pixels
Median diameter	212.6 pixels
90th pctile diameter	212.6 pixels
Thresholding filter size	0.0
Area covered by objects	1.0 %

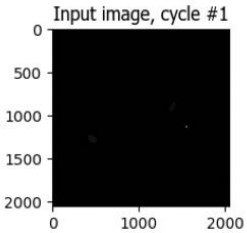

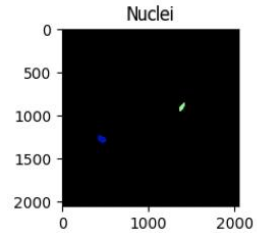

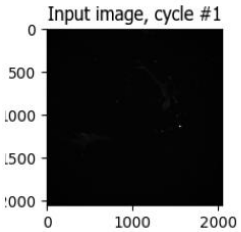

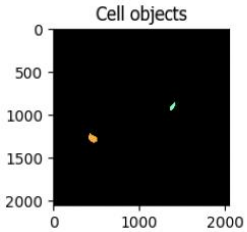

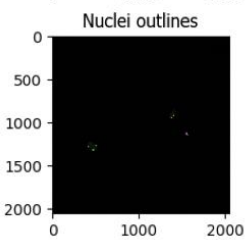

# of accepted objects	2
10th pctile diameter	65.9 pixels
Median diameter	92.7 pixels
90th pctile diameter	92.7 pixels
Area covered by objects	0.2 %
Thresholding filter size	1.0
Threshold	0.0184

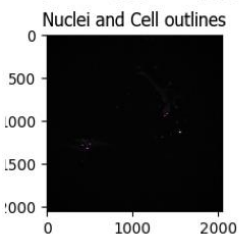

Threshold	0.0412
10th pctile diameter	66.0 pixels
Median diameter	94.2 pixels
90th pctile diameter	94.2 pixels
Thresholding filter size	0.0
Area covered by objects	0.2 %

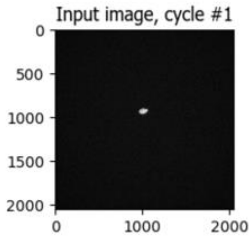

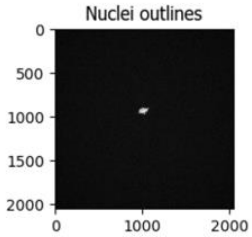

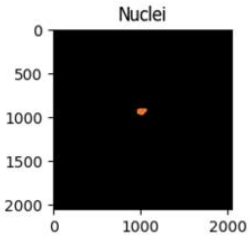

# of accepted objects	1
10th pctile diameter	95.6 pixels
Median diameter	95.6 pixels
90th pctile diameter	95.6 pixels
Area covered by objects	0.2 %
Thresholding filter size	1.0
Threshold	0.00716

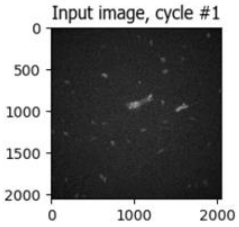

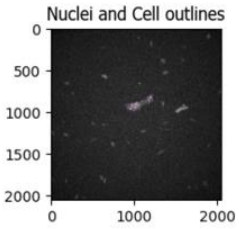

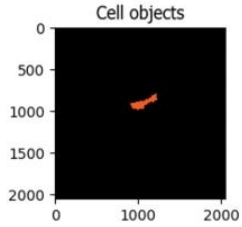

Threshold	0.0191
10th pctile diameter	174.6 pixels
Median diameter	174.6 pixels
90th pctile diameter	174.6 pixels
Thresholding filter size	0.0
Area covered by objects	0.6 %

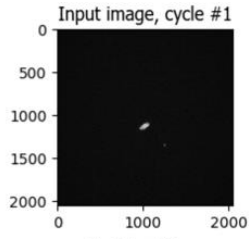

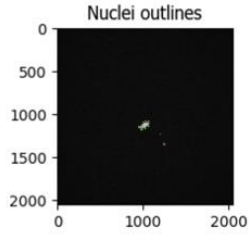

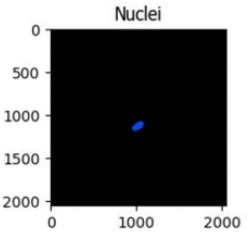

# of accepted objects	1
10th pctile diameter	108.6 pixels
Median diameter	108.6 pixels
90th pctile diameter	108.6 pixels
Area covered by objects	0.2 %
Thresholding filter size	1.0
Threshold	0.00736

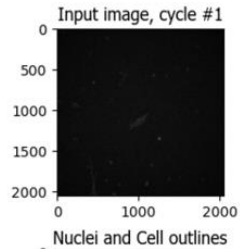

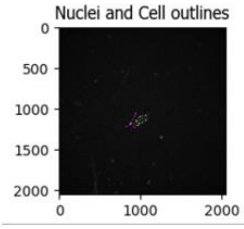

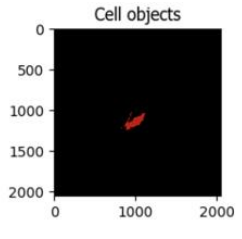

Threshold	0.0181
10th pctile diameter	172.6 pixels
Median diameter	172.6 pixels
90th pctile diameter	172.6 pixels
Thresholding filter size	0.0
Area covered by objects	0.6 %

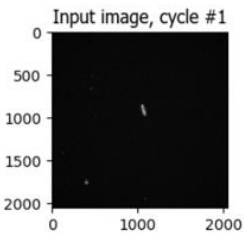

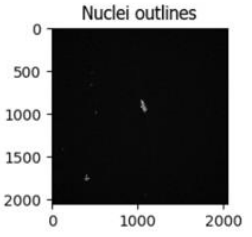

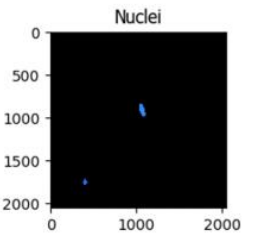

# of accepted objects	2
10th pctile diameter	56.0 pixels
Median diameter	98.5 pixels
90th pctile diameter	98.5 pixels
Area covered by objects	0.2 %
Thresholding filter size	1.0
Threshold	0.00728

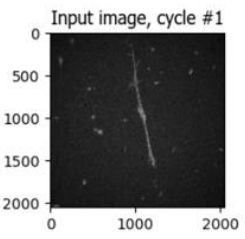

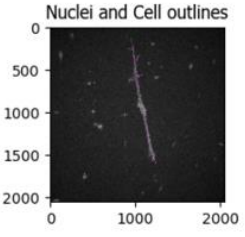

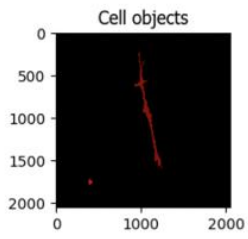

Threshold	0.0191
10th pctile diameter	56.2 pixels
Median diameter	255.8 pixels
90th pctile diameter	255.8 pixels
Thresholding filter size	0.0
Area covered by objects	1.3 %

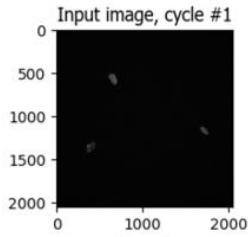

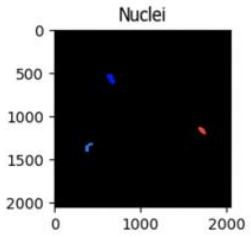

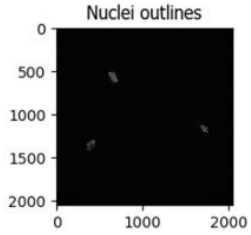

# of accepted objects	3
10th pctile diameter	75.5 pixels
Median diameter	75.9 pixels
90th pctile diameter	100.0 pixels
Area covered by objects	0.4 %
Thresholding filter size	1.0
Threshold	0.0164

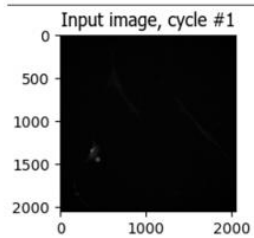

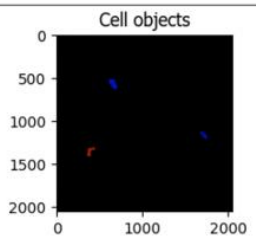

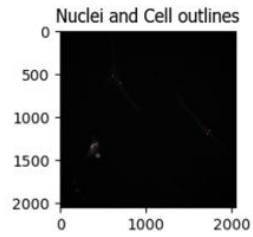

Threshold	0.0531
10th pctile diameter	75.5 pixels
Median diameter	83.3 pixels
90th pctile diameter	100.0 pixels
Thresholding filter size	0.0
Area covered by objects	0.4 %

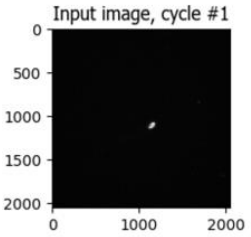

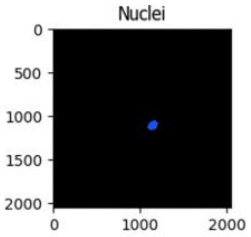

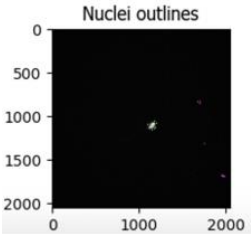

# of accepted objects	1
10th pctile diameter	110.4 pixels
Median diameter	110.4 pixels
90th pctile diameter	110.4 pixels
Area covered by objects	0.2 %
Thresholding filter size	1.0
Threshold	0.0076

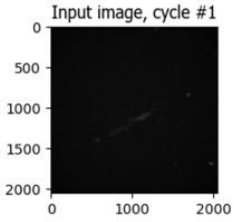

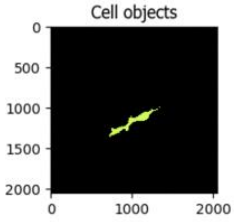

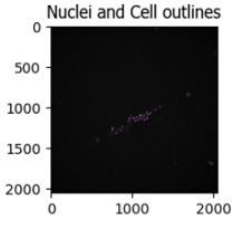

Threshold	0.0188
10th pctile diameter	217.9 pixels
Median diameter	217.9 pixels
90th pctile diameter	217.9 pixels
Thresholding filter size	0.0
Area covered by objects	0.9 %

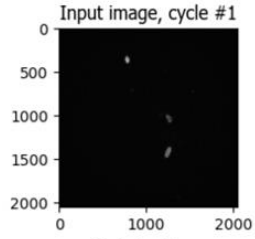

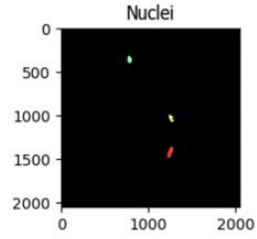

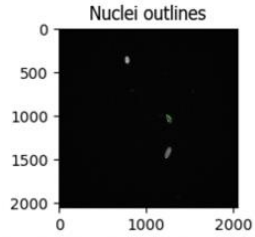

# of accepted objects	3
10th pctile diameter	63.8 pixels
Median diameter	64.4 pixels
90th pctile diameter	85.4 pixels
Area covered by objects	0.3 %
Thresholding filter size	1.0
Threshold	0.0214

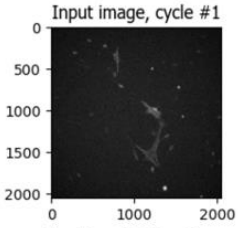

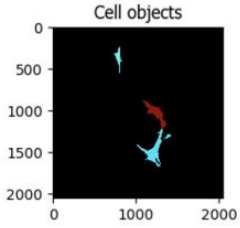

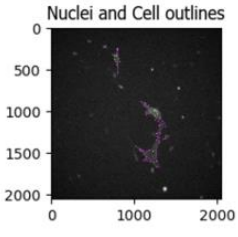

Threshold	0.0179
10th pctile diameter	110.8 pixels
Median diameter	193.1 pixels
90th pctile diameter	220.7 pixels
Thresholding filter size	0.0
Area covered by objects	1.8 %

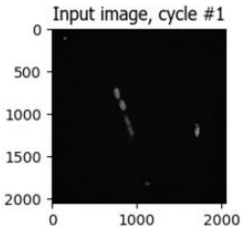

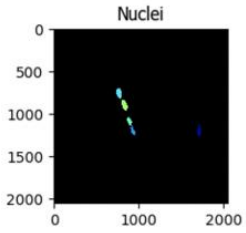

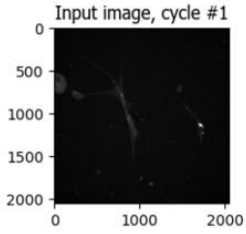

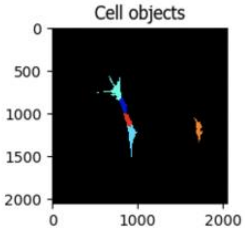

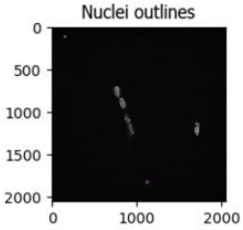

# of accepted objects	5
10th pctile diameter	66.1 pixels
Median diameter	81.9 pixels
90th pctile diameter	89.3 pixels
Area covered by objects	0.6 %
Thresholding filter size	1.0
Threshold	0.0178

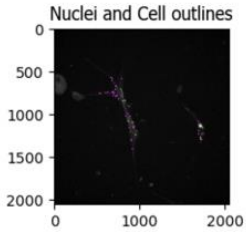

Threshold	0.0229
10th pctile diameter	106.2 pixels
Median diameter	120.6 pixels
90th pctile diameter	159.3 pixels
Thresholding filter size	0.0
Area covered by objects	1.6 %

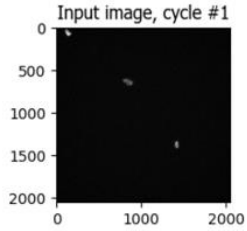

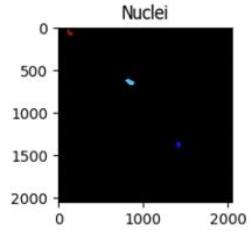

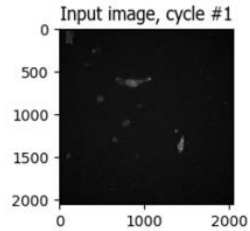

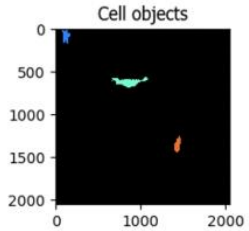

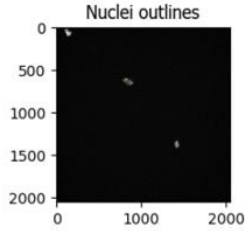

# of accepted objects	3
10th pctile diameter	57.2 pixels
Median diameter	67.8 pixels
90th pctile diameter	78.4 pixels
Area covered by objects	0.3 %
Thresholding filter size	1.0
Threshold	0.0206

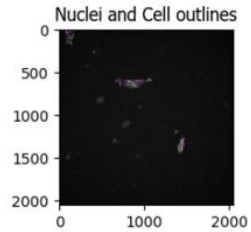

Threshold	0.0214
10th pctile diameter	111.5 pixels
Median diameter	117.3 pixels
90th pctile diameter	176.0 pixels
Thresholding filter size	0.0
Area covered by objects	1.1 %

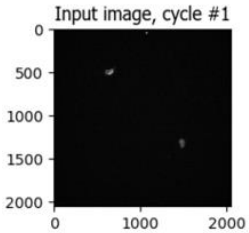

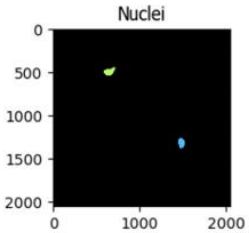

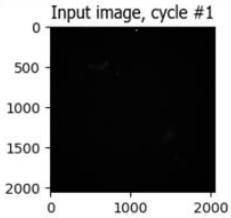

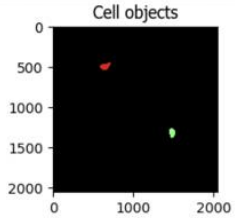

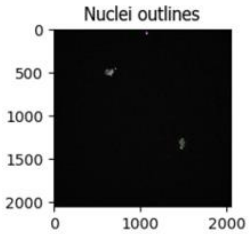

# of accepted objects	2
10th pctile diameter	94.6 pixels
Median diameter	103.5 pixels
90th pctile diameter	103.5 pixels
Area covered by objects	0.4 %
Thresholding filter size	1.0
Threshold	0.00741

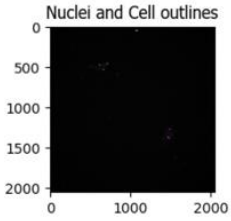

Threshold	0.123
10th pctile diameter	94.6 pixels
Median diameter	103.5 pixels
90th pctile diameter	103.5 pixels
Thresholding filter size	0.0
Area covered by objects	0.4 %

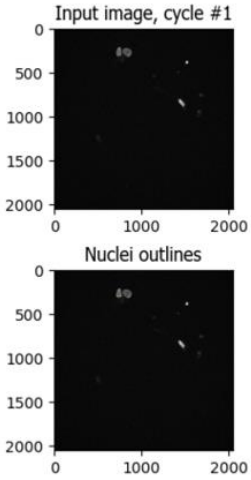

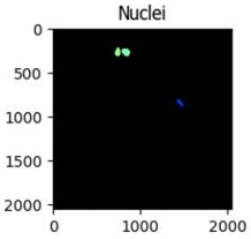

# of accepted objects	3
10th pctile diameter	65.5 pixels
Median diameter	77.6 pixels
90th pctile diameter	95.3 pixels
Area covered by objects	0.4 %
Thresholding filter size	1.0
Threshold	0.0175

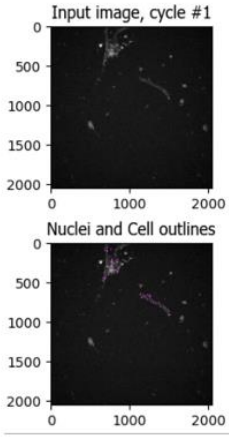

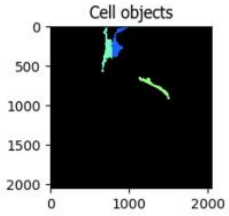

Threshold	0.0185
10th pctile diameter	159.9 pixels
Median diameter	188.8 pixels
90th pctile diameter	204.9 pixels
Thresholding filter size	0.0
Area covered by objects	1.9 %

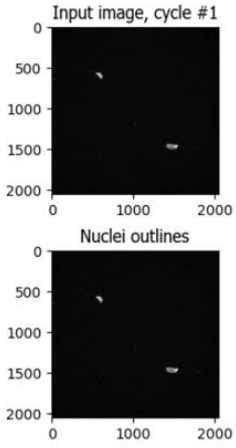

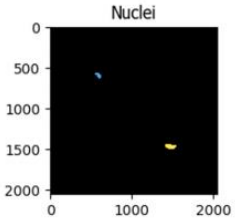

# of accepted objects	2
10th pctile diameter	62.8 pixels
Median diameter	90.5 pixels
90th pctile diameter	90.5 pixels
Area covered by objects	0.2 %
Thresholding filter size	1.0
Threshold	0.0207

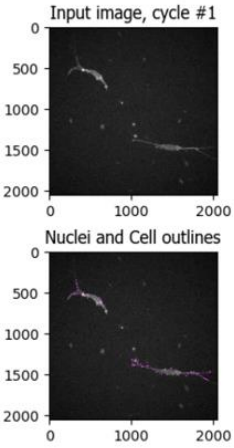

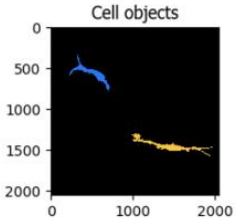

Threshold	0.0173
10th pctile diameter	207.5 pixels
Median diameter	236.6 pixels
90th pctile diameter	236.6 pixels
Thresholding filter size	0.0
Area covered by objects	1.9 %

CellProfiler Images of Live Cells: 10% PMMA Cells

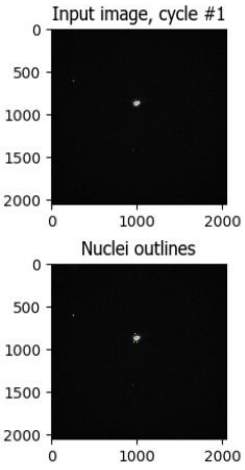

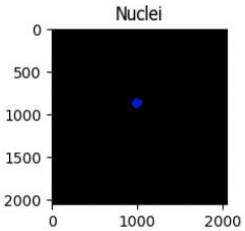

# of accepted objects	1
10th pctile diameter	114.4 pixels
Median diameter	114.4 pixels
90th pctile diameter	114.4 pixels
Area covered by objects	0.2 %
Thresholding filter size	1.0
Threshold	0.00732

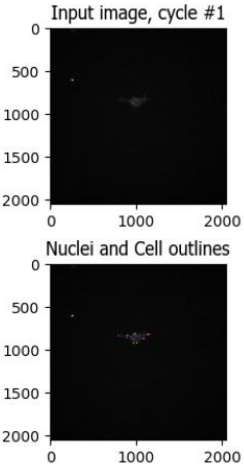

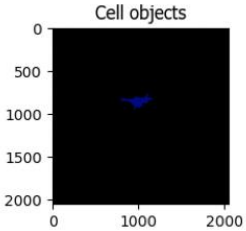

Threshold	0.0207
10th pctile diameter	176.1 pixels
Median diameter	176.1 pixels
90th pctile diameter	176.1 pixels
Thresholding filter size	0.0
Area covered by objects	0.6 %

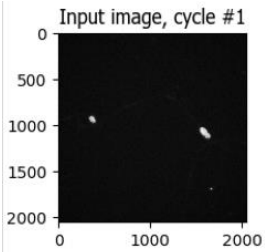

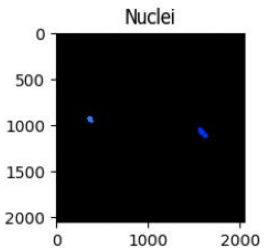

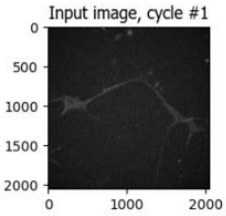

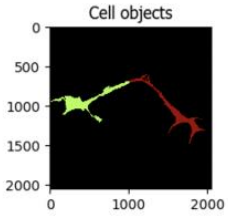

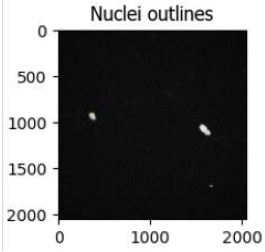

# of accepted objects	2
10th pctile diameter	67.9 pixels
Median diameter	98.7 pixels
90th pctile diameter	98.7 pixels
Area covered by objects	0.3 %
Thresholding filter size	1.0
Threshold	0.0205

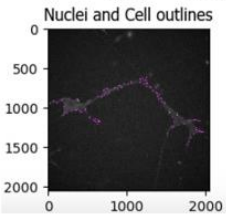

Threshold	0.0173
10th pctile diameter	308.4 pixels
Median diameter	315.7 pixels
90th pctile diameter	315.7 pixels
Thresholding filter size	0.0
Area covered by objects	3.6 %

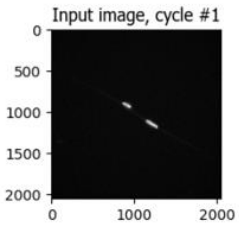

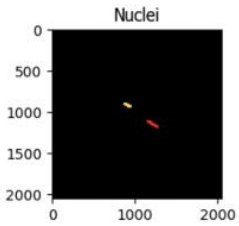

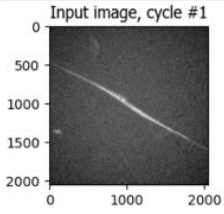

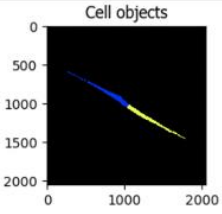

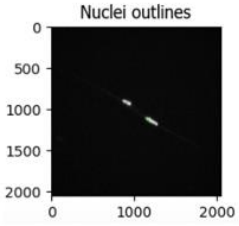

# of accepted objects	2
10th pctile diameter	72.9 pixels
Median diameter	90.1 pixels
90th pctile diameter	90.1 pixels
Area covered by objects	0.3 %
Thresholding filter size	1.0
Threshold	0.0208

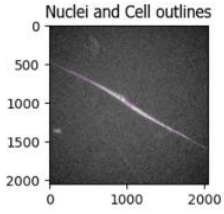

Threshold	0.0196
10th pctile diameter	189.0 pixels
Median diameter	194.0 pixels
90th pctile diameter	194.0 pixels
Thresholding filter size	0.0
Area covered by objects	1.4 %

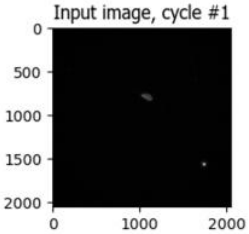

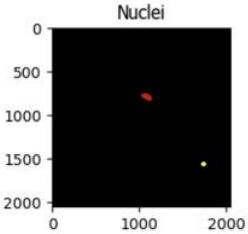

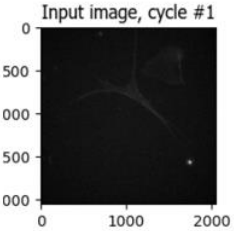

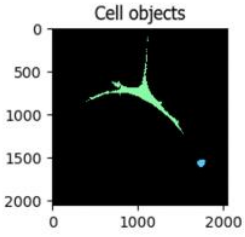

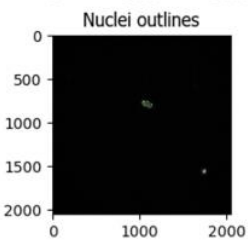

# of accepted objects	2
10th pctile diameter	55.8 pixels
Median diameter	95.8 pixels
90th pctile diameter	95.8 pixels
Area covered by objects	0.2 %
Thresholding filter size	1.0
Threshold	0.0269

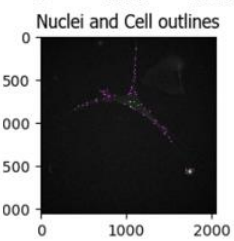

Threshold	0.0185
10th pctile diameter	90.6 pixels
Median diameter	338.1 pixels
90th pctile diameter	338.1 pixels
Thresholding filter size	0.0
Area covered by objects	2.3 %

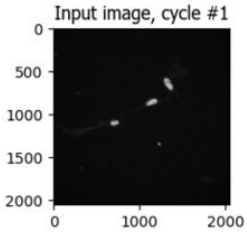

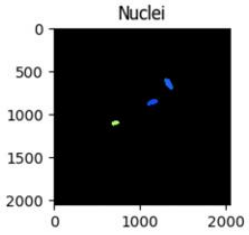

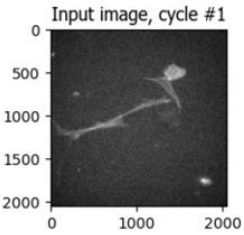

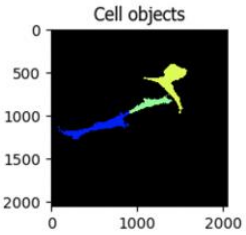

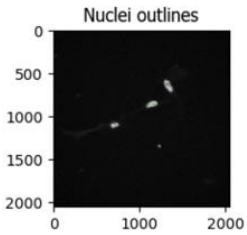

# of accepted objects	3
10th pctile diameter	70.2 pixels
Median diameter	89.0 pixels
90th pctile diameter	104.0 pixels
Area covered by objects	0.4 %
Thresholding filter size	1.0
Threshold	0.0184

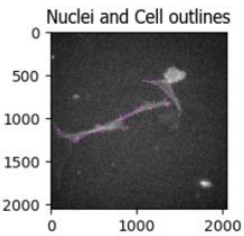

Threshold	0.0179
10th pctile diameter	205.2 pixels
Median diameter	286.7 pixels
90th pctile diameter	309.7 pixels
Thresholding filter size	0.0
Area covered by objects	4.1 %

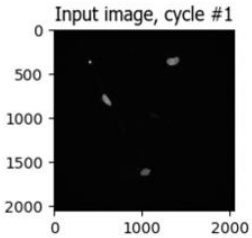

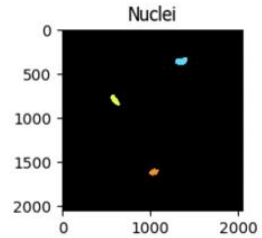

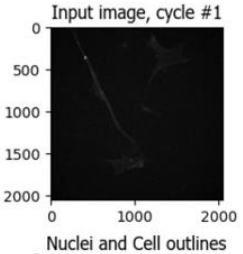

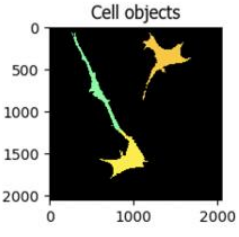

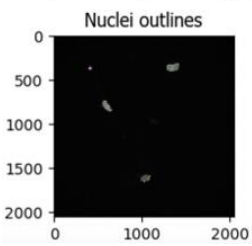

# of accepted objects	3
10th pctile diameter	88.2 pixels
Median diameter	96.5 pixels
90th pctile diameter	110.5 pixels
Area covered by objects	0.5 %
Thresholding filter size	1.0
Threshold	0.0251

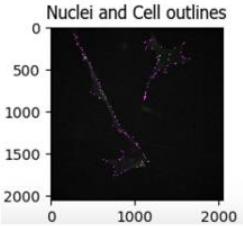

Threshold	0.0175
10th pctile diameter	289.5 pixels
Median diameter	351.0 pixels
90th pctile diameter	356.5 pixels
Thresholding filter size	0.0
Area covered by objects	6.3 %

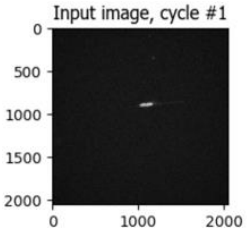

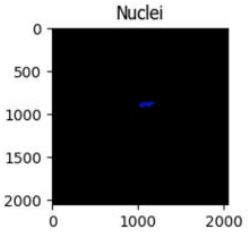

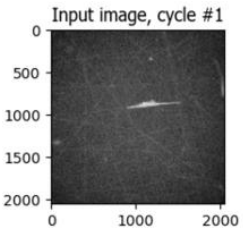

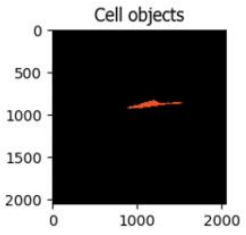

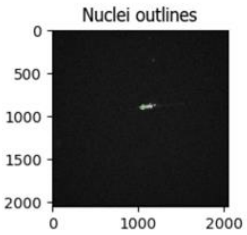

# of accepted objects	1
10th pctile diameter	102.8 pixels
Median diameter	102.8 pixels
90th pctile diameter	102.8 pixels
Area covered by objects	0.2 %
Thresholding filter size	1.0
Threshold	0.00727

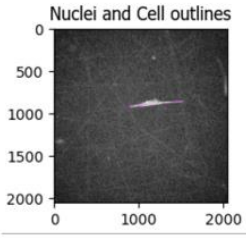

Threshold	0.0191
10th pctile diameter	176.0 pixels
Median diameter	176.0 pixels
90th pctile diameter	176.0 pixels
Thresholding filter size	0.0
Area covered by objects	0.6 %

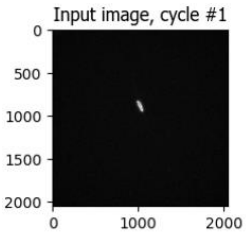

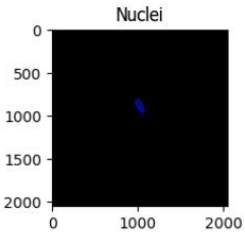

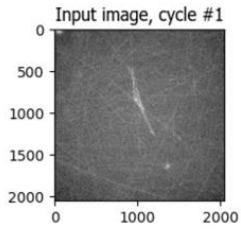

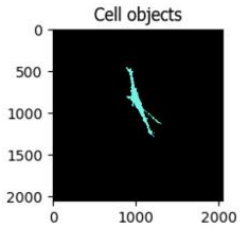

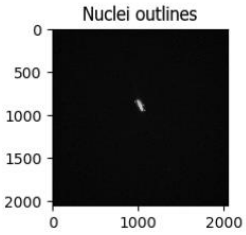

# of accepted objects	1
10th pctile diameter	127.0 pixels
Median diameter	127.0 pixels
90th pctile diameter	127.0 pixels
Area covered by objects	0.3 %
Thresholding filter size	1.0
Threshold	0.00739

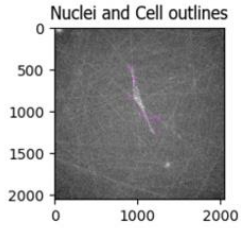

Threshold	0.0177
10th pctile diameter	253.1 pixels
Median diameter	253.1 pixels
90th pctile diameter	253.1 pixels
Thresholding filter size	0.0
Area covered by objects	1.2 %

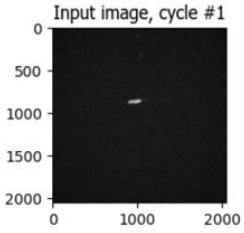

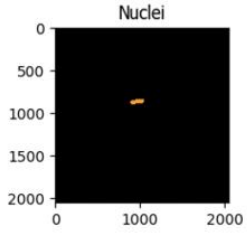

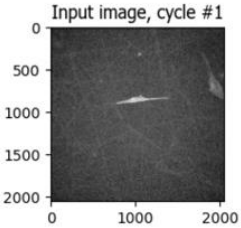

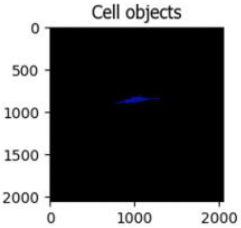

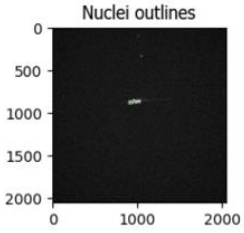

# of accepted objects	1
10th pctile diameter	97.3 pixels
Median diameter	97.3 pixels
90th pctile diameter	97.3 pixels
Area covered by objects	0.2 %
Thresholding filter size	1.0
Threshold	0.00722

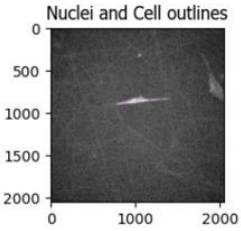

Threshold	0.0232
10th pctile diameter	146.3 pixels
Median diameter	146.3 pixels
90th pctile diameter	146.3 pixels
Thresholding filter size	0.0
Area covered by objects	0.4 %

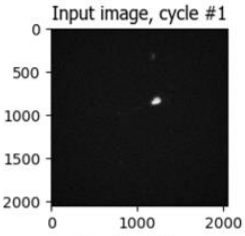

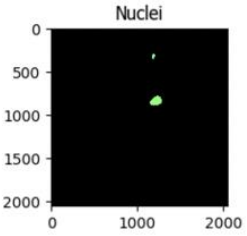

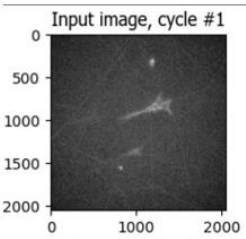

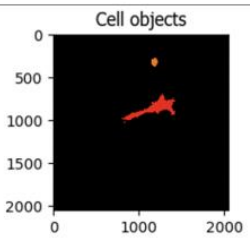

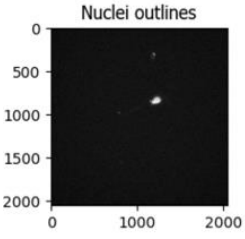

# of accepted objects	2
10th pctile diameter	46.1 pixels
Median diameter	121.8 pixels
90th pctile diameter	121.8 pixels
Area covered by objects	0.3 %
Thresholding filter size	1.0
Threshold	0.00723

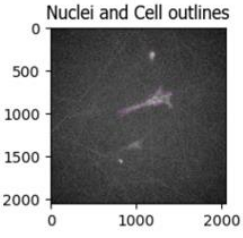

Threshold	0.018
10th pctile diameter	84.3 pixels
Median diameter	266.0 pixels
90th pctile diameter	266.0 pixels
Thresholding filter size	0.0
Area covered by objects	1.5 %

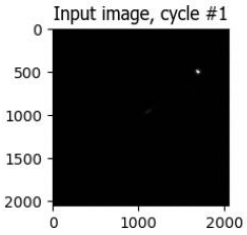

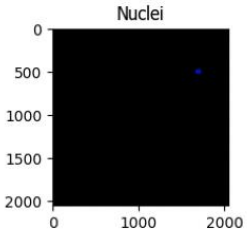

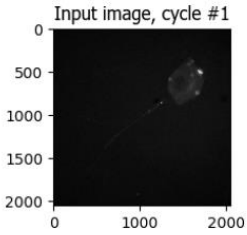

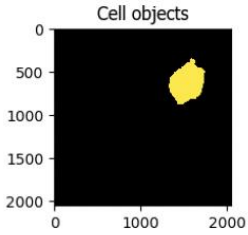

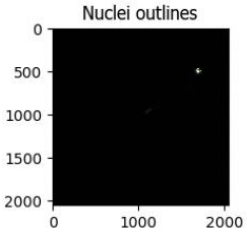

# of accepted objects	1
10th pctile diameter	64.0 pixels
Median diameter	64.0 pixels
90th pctile diameter	64.0 pixels
Area covered by objects	0.1 %
Thresholding filter size	1.0
Threshold	0.0354

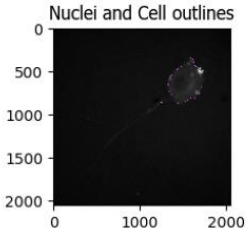

Threshold	0.0235
10th pctile diameter	432.2 pixels
Median diameter	432.2 pixels
90th pctile diameter	432.2 pixels
Thresholding filter size	0.0
Area covered by objects	3.5 %

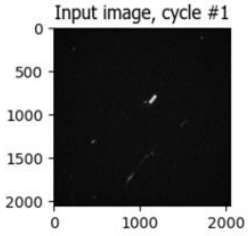

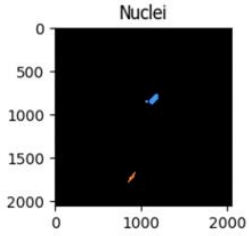

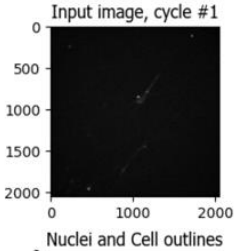

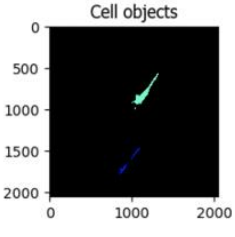

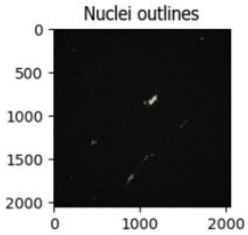

# of accepted objects	2
10th pctile diameter	67.3 pixels
Median diameter	101.6 pixels
90th pctile diameter	101.6 pixels
Area covered by objects	0.3 %
Thresholding filter size	1.0
Threshold	0.00725

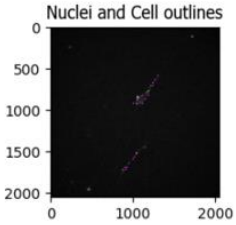

Threshold	0.0191
10th pctile diameter	94.4 pixels
Median diameter	164.2 pixels
90th pctile diameter	164.2 pixels
Thresholding filter size	0.0
Area covered by objects	0.7 %

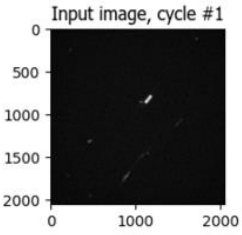

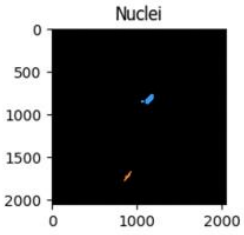

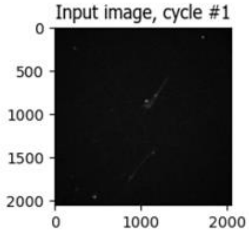

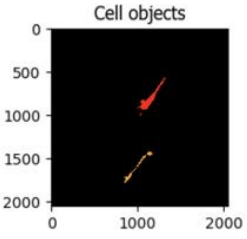

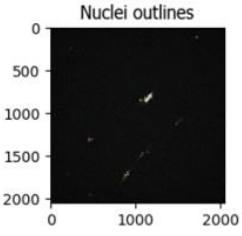

# of accepted objects	2
10th pctile diameter	67.3 pixels
Median diameter	101.6 pixels
90th pctile diameter	101.6 pixels
Area covered by objects	0.3 %
Thresholding filter size	1.0
Threshold	0.00725

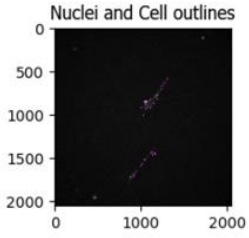

Threshold	0.0187
10th pctile diameter	112.4 pixels
Median diameter	167.3 pixels
90th pctile diameter	167.3 pixels
Thresholding filter size	0.0
Area covered by objects	0.8 %

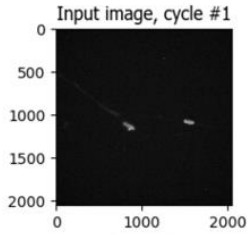

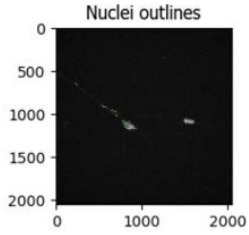

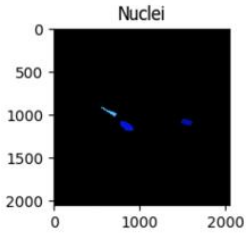

# of accepted objects	3
10th pctile diameter	80.5 pixels
Median diameter	95.7 pixels
90th pctile diameter	121.7 pixels
Area covered by objects	0.6 %
Thresholding filter size	1.0
Threshold	0.00681

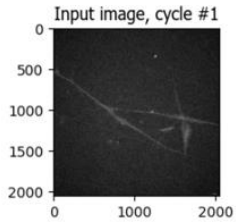

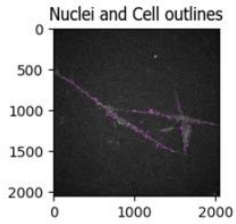

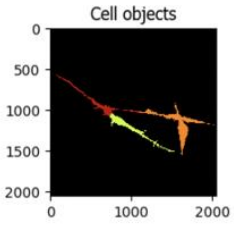

Threshold	0.0175
10th pctile diameter	209.9 pixels
Median diameter	212.0 pixels
90th pctile diameter	288.3 pixels
Thresholding filter size	0.0
Area covered by objects	3.2 %

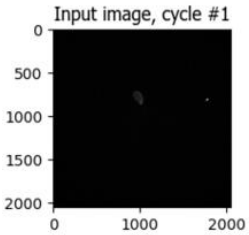

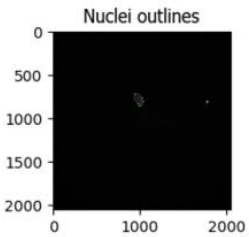

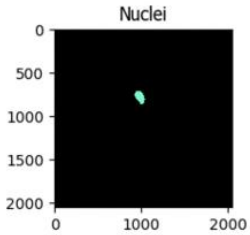

# of accepted objects	1
10th pctile diameter	124.1 pixels
Median diameter	124.1 pixels
90th pctile diameter	124.1 pixels
Area covered by objects	0.3 %
Thresholding filter size	1.0
Threshold	0.0181

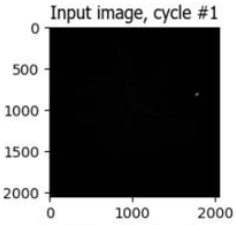

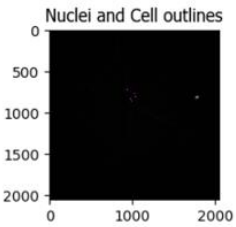

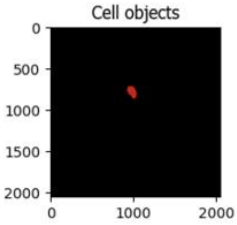

Threshold	0.431
10th pctile diameter	124.1 pixels
Median diameter	124.1 pixels
90th pctile diameter	124.1 pixels
Thresholding filter size	0.0
Area covered by objects	0.3 %

Appendix B: DIC Images of Cells on Surfaces

Flat Surface DIC Images of Live Cells

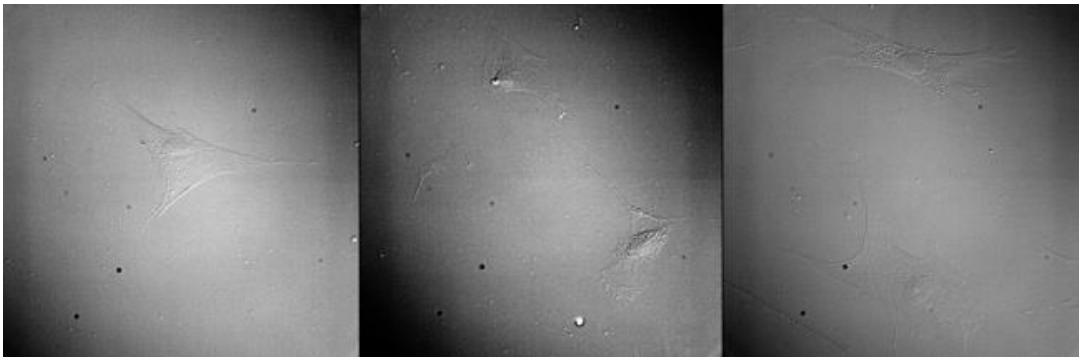

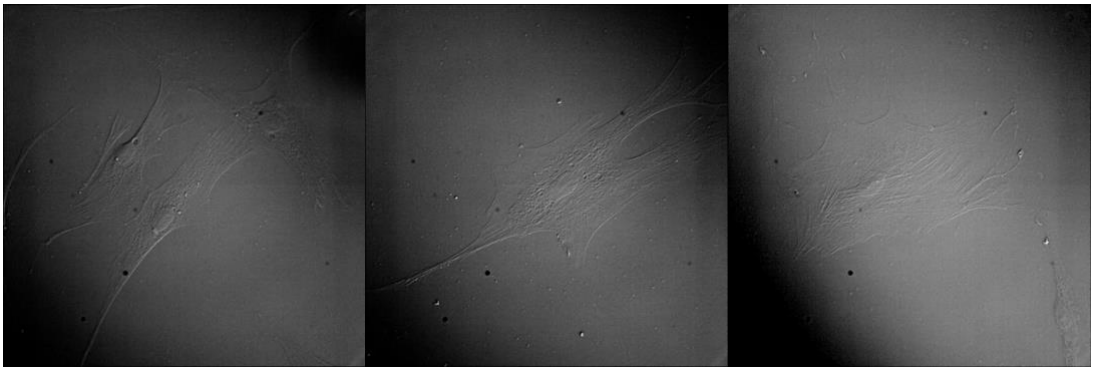

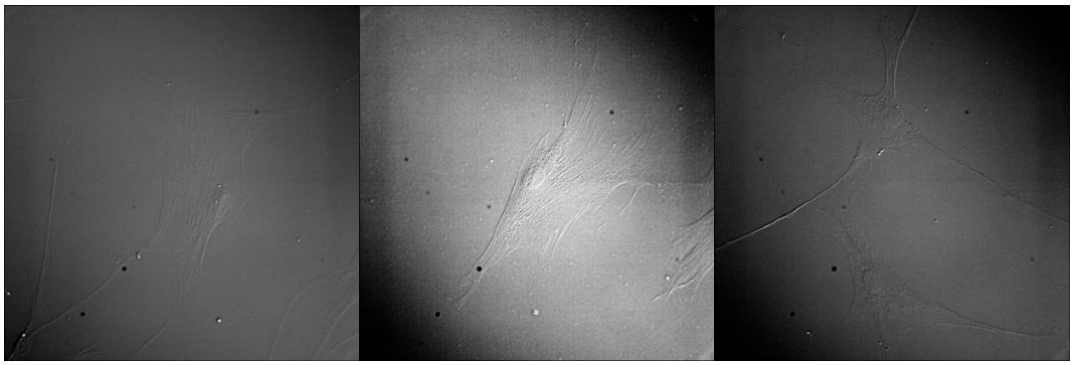

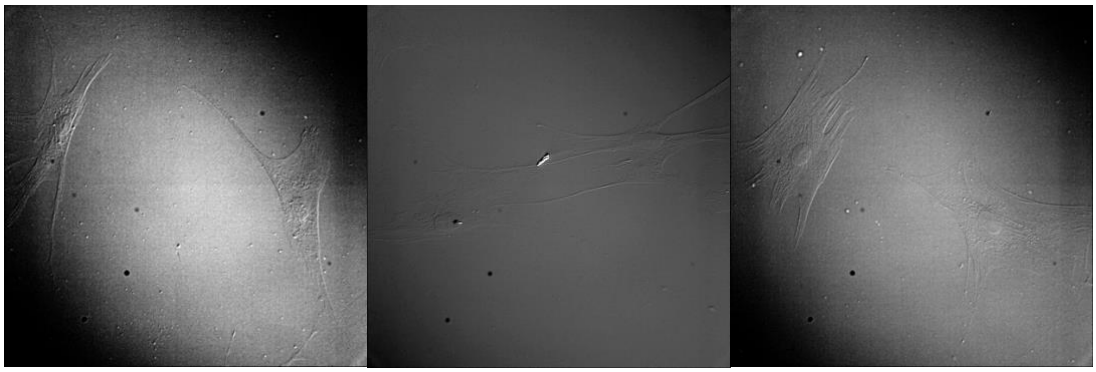

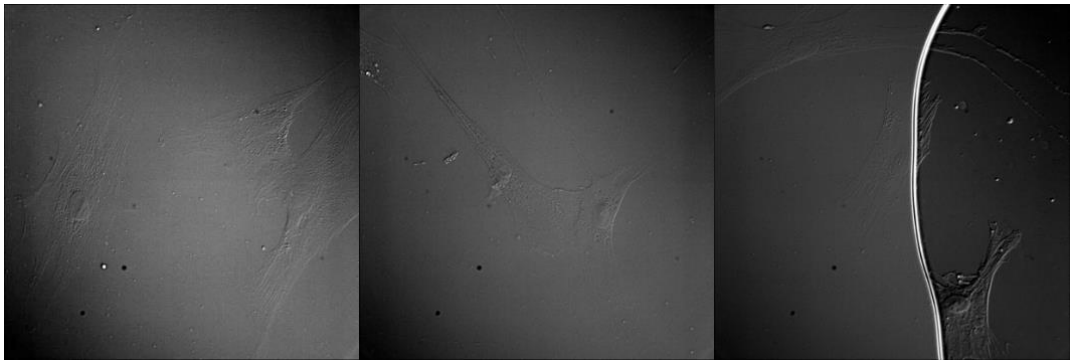

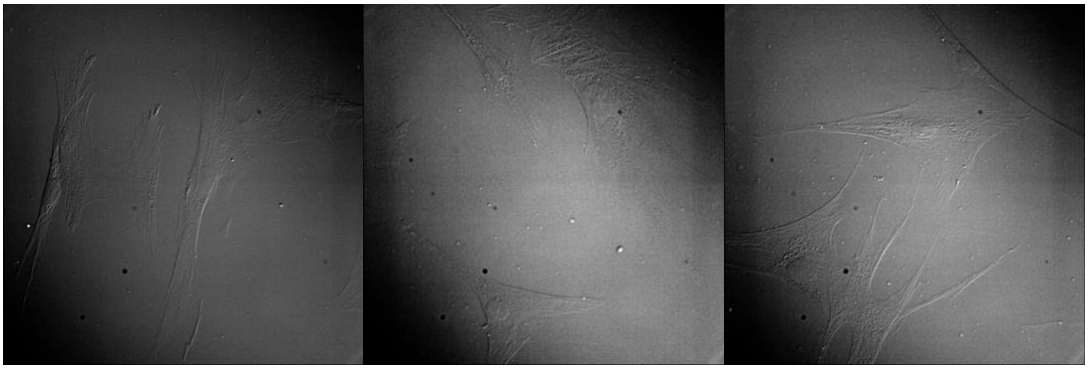

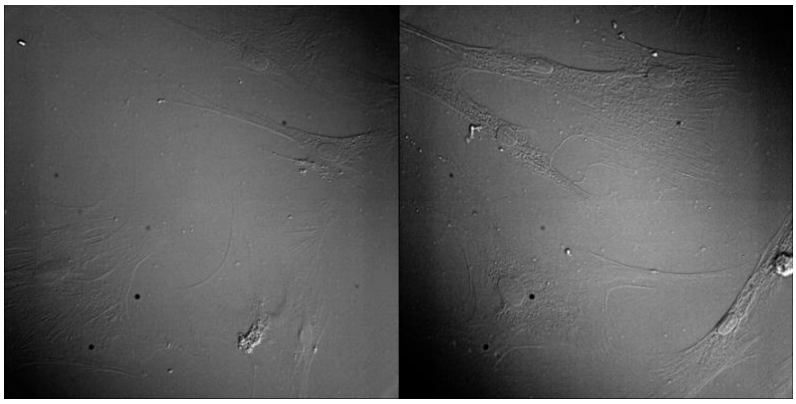

5% PMMA DIC Images of Live Cells and Fibers

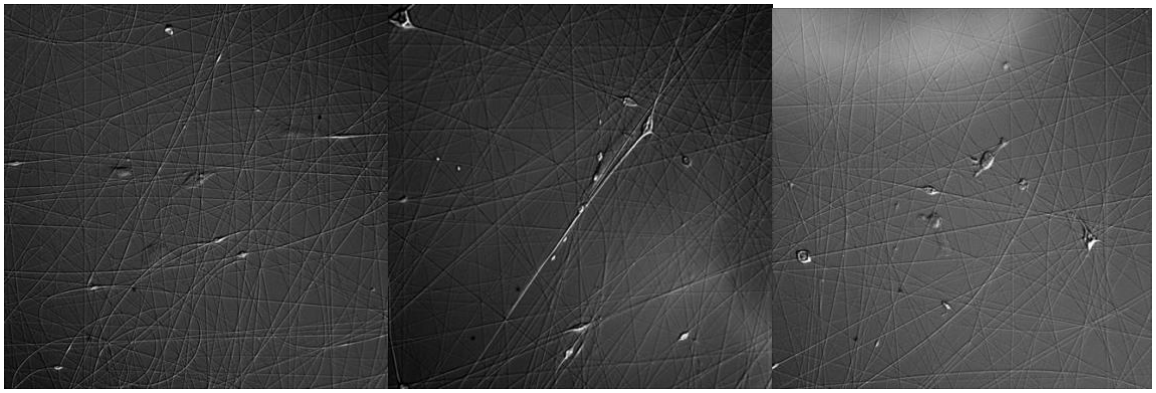

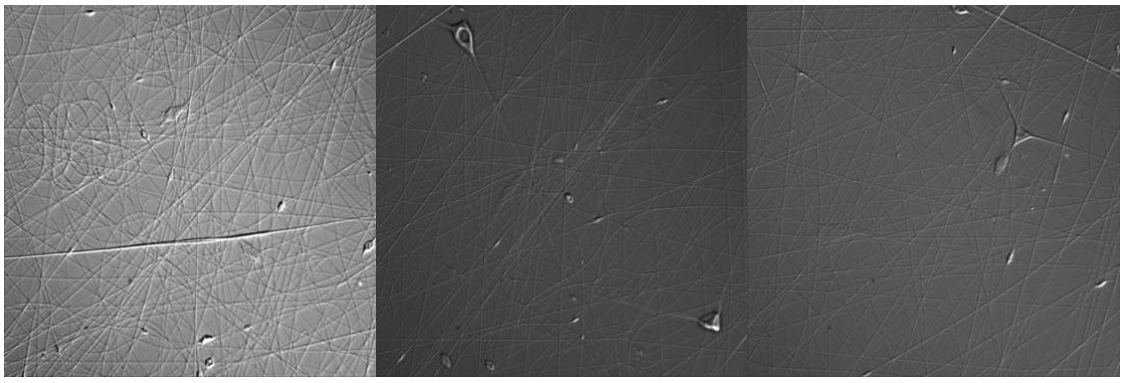

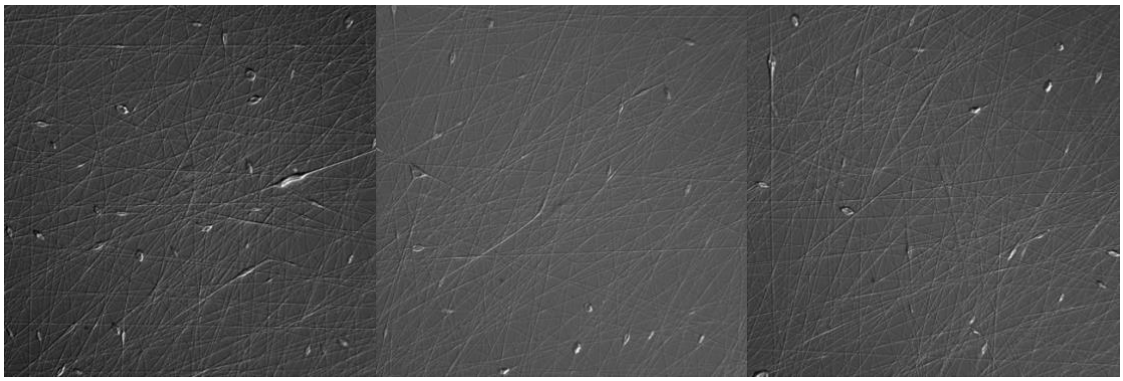

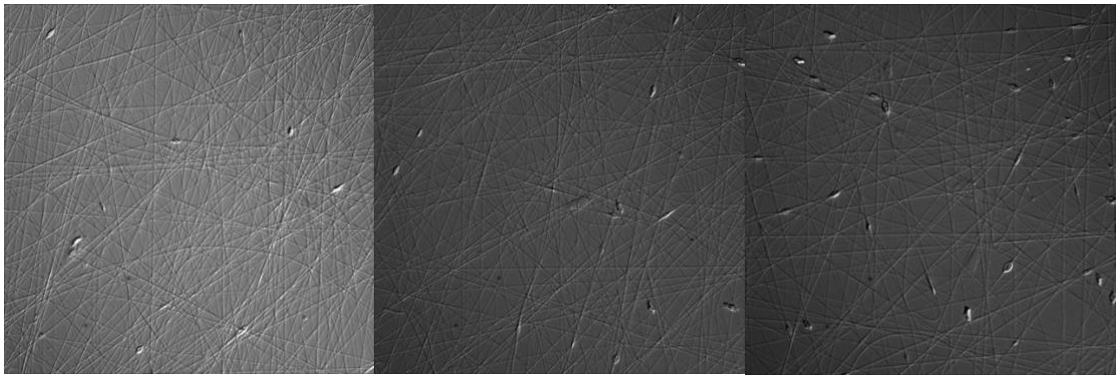

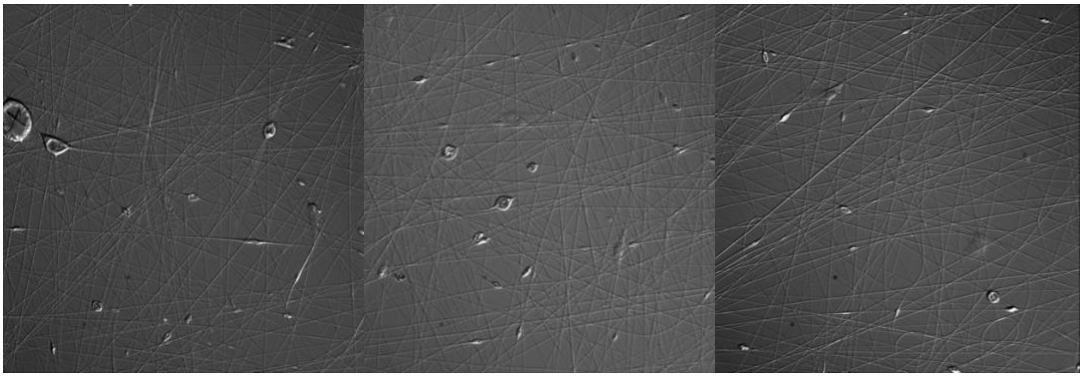

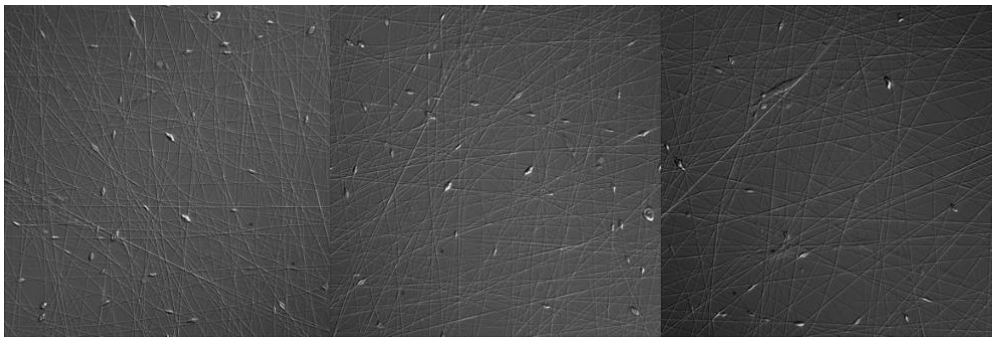

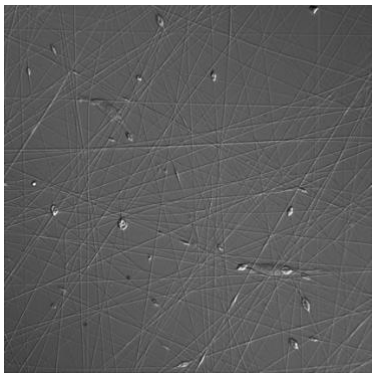

10% PMMA DIC Images of Live Cells and Fibers

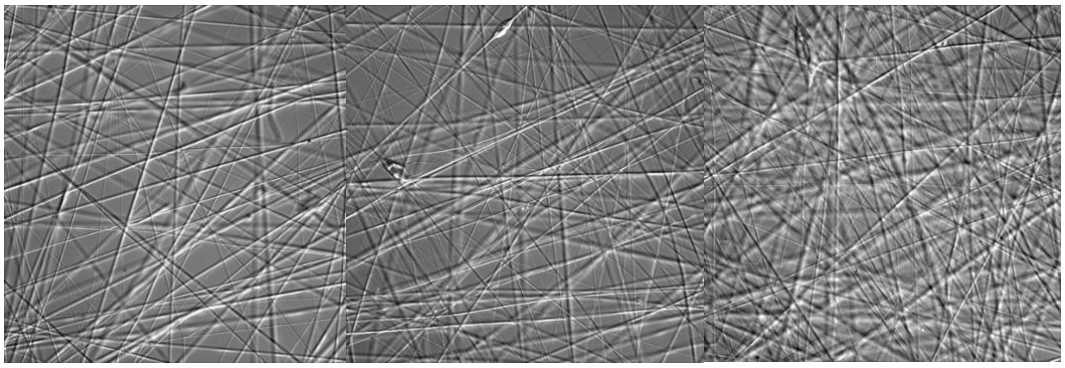

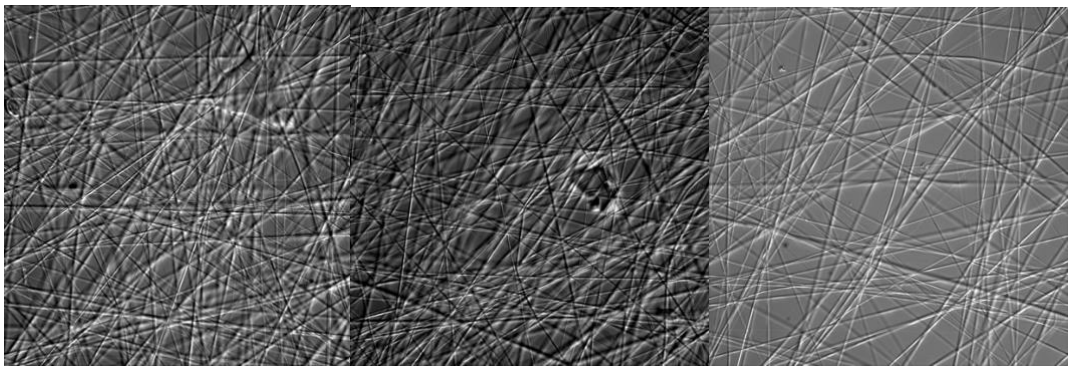

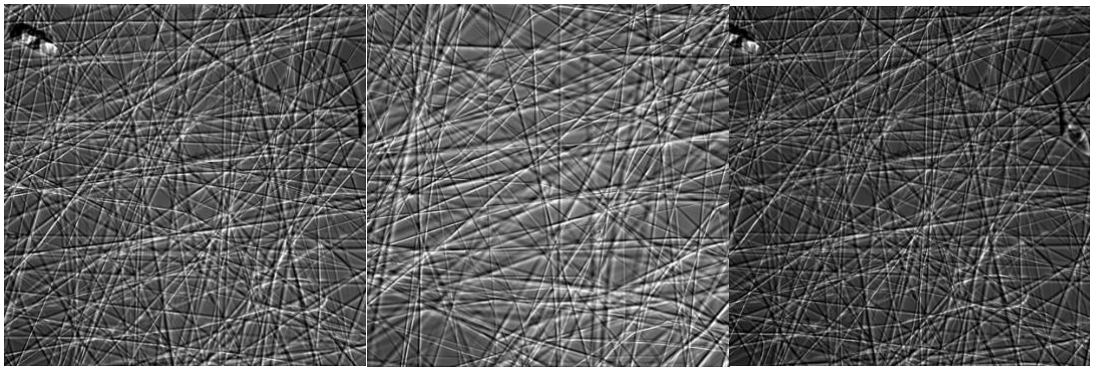

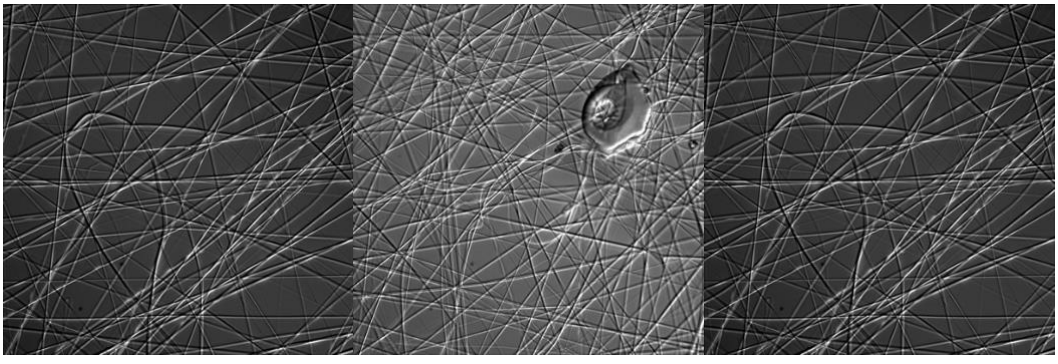

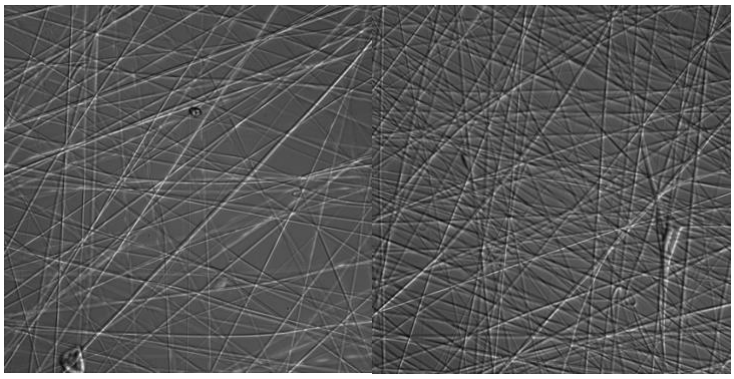

BIBLIOGRAPHY

[1] "Stem Cell Research," *Mayo Clinic*, 08-Jun-2019. [Online]. Available: https://www.mayoclinic.org/tests-procedures/bone-marrow-transplant/in-depth/stem-cells/art-20048117. [Accessed: 05-Jan-2021].

[2] I. Ullah, R. B. Subbarao, and G. J. Rho, "Human mesenchymal stem cells - current trends and future prospective," *Bioscience reports*, 28-Apr-2015. [Online]. Available: https://www.ncbi.nlm.nih.gov/pmc/articles/PMC4413017/. [Accessed: 05-Jan-2021].

[3] M. Malumbres, "Control of the Cell Cycle," *Abeloff's Clinical Oncology (Fifth Edition)*, 28-Aug-2013. [Online]. Available: https://www.sciencedirect.com/science/article/pii/B9781455728657000047. [Accessed: 07-Jan-2021].

[4] H. Lodish, "Overview of the Cell Cycle and Its Control," *Molecular Cell Biology. 4th edition.*, 01-Jan-1970. [Online]. Available: https://www.ncbi.nlm.nih.gov/books/NBK21466/. [Accessed: 07-Jan-2021].

[5] Y. Gruenbaum, R. D. Goldman, R. Meyuhas, E. Mills, A. Margalit, A. Fridkin, Y. Dayani, M. Prokocimer, and A. Enosh, "The Nuclear Lamina and its Functions in the Nucleus," *International review of cytology*. [Online]. Available: https://pubmed.ncbi.nlm.nih.gov/12921235/#:~:text=The%20nuclear%20lamina%20is%20a,membrane%20and%20the%20peripheral%20chromatin.&text=It%20is%20involved%20in%20most,%2C%20nuclear%20migration%2C%20and%20apoptosis. [Accessed: 07-Jan-2021].

[6] P. M. Davidson and J. Lammerding, "Broken nuclei--lamins, nuclear mechanics, and disease," *National Center for Biotechnology Information*, 02-Dec-2013. [Online]. Available: https://pubmed.ncbi.nlm.nih.gov/24309562/. [Accessed: 07-Feb-2021].

[7] I. Rajagopal, "The Nuclear Envelope and traffic between the nucleus and cytoplasm.," *Oregon State University*, 2009. [Online]. Available: http://oregonstate.edu/instruction/bi314/summer09/nucleus.html. [Accessed: 07-Feb-2021].

[8] E. Torvaldson, V. Kochin, and J. E. Eriksson, "Phosphorylation of lamins determine their structural properties and signaling functions," *US National Library of Medicine*, 2015. [Online]. Available: https://www.ncbi.nlm.nih.gov/pmc/articles/PMC4615644/. [Accessed: 13-Mar-2021].

[9] T. Dechat, S. A. Adam, P. Taimen, T. Shimi, and R. D. Goldman, "Nuclear lamins," *Cold Spring Harbor perspectives in biology*, Nov-2010. [Online]. Available: https://www.ncbi.nlm.nih.gov/pmc/articles/PMC2964183/#A000547C172. [Accessed: 14-Mar-2021].

[10] S. Y. Liu and K. Ikegami, “Nuclear lamin phosphorylation: an emerging role in gene regulation and pathogenesis of laminopathies,” *Nucleus (Austin, Tex.)*, Dec-2020. [Online]. Available: https://www.ncbi.nlm.nih.gov/pmc/articles/PMC7588210/. [Accessed: 15-Mar-2021].

[11] D. Howard, L. D. Buttery, K. M. Shakesheff, and S. J. Roberts, “Tissue engineering: strategies, stem cells and scaffolds,” *NCBI: Journal of Anatomy*, Jul-2008. [Online]. Available: https://www.ncbi.nlm.nih.gov/pmc/articles/PMC2475566/. [Accessed: 07-Feb-2021].

[12] I. Jun, H.-S. Han, J. R. Edwards, and H. Jeon, “Electrospun Fibrous Scaffolds for Tissue Engineering: Viewpoints on Architecture and Fabrication,” *International Journal of Molecular Sciences*, 06-Mar-2018. [Online]. Available: http://www.ncbi.nlm.nih.gov/pmc/articles/PMC5877606/. [Accessed: 07-Feb-2021].

[13] N. Zhu and X. Chen , *Electrospinning Process* . https://www.intechopen.com/books/advances-in-biomaterials-science-and-biomedical-applications/biofabrication-of-tissue-scaffolds, 2013.

[14] J. Fan, Y. Zhang, Y. Liu, Y. Wang, F. Cao, Q. Yang, and F. Tian, “Explanation of the cell orientation in a nanofiber membrane by the geometric potential theory,” *Results in Physics*, 31-Jul-2019. [Online]. Available: https://www.sciencedirect.com/science/article/pii/S2211379719319643. [Accessed: 12-Feb-2021].

[15] D. P. Ura, J. E. Karbowniczek, P. K. Szewczyk, S. Metwally, M. Kopyściański, and U. Stachewicz, “Cell Integration with Electrospun PMMA Nanofibers, Microfibers, Ribbons, and Films: A Microscopy Study,” *Bioengineering (Basel, Switzerland)*, 09-May-2019. [Online]. Available: https://www.ncbi.nlm.nih.gov/pmc/articles/PMC6630608/. [Accessed: 20-Feb-2021].

[16] “How to Label Antibodies,” *MBL: International Corporation*, 04-Aug-2020. [Online]. Available: https://www.mblintl.com/resources/scientific-resources/fundamentals-for-planning-research/how-to-label-antibodies/. [Accessed: 09-Mar-2021].

[17] “Phospho-Lamin A/C (Ser22) Antibody,” *Cell Signaling Technology*. [Online]. Available: https://www.cellsignal.com/products/primary-antibodies/phospho-lamin-a-c-ser22-antibody/2026?Ns=product.sortId%7C0&N=102236%2B4294956287&fromPage=plp. [Accessed: 14-Mar-2021].

[18] “Alexa Fluor 568 dye,” *Thermo Fisher Scientific - US*. [Online]. Available: https://www.thermofisher.com/us/en/home/life-science/cell-analysis/fluorophores/alexa-fluor-568.html. [Accessed: 09-Mar-2021].

[19] “Alexa Fluor 488 dye,” *Thermo Fisher Scientific - US*. [Online]. Available: https://www.thermofisher.com/us/en/home/life-science/cell-analysis/fluorophores/alexa-fluor-488.html. [Accessed: 09-Mar-2021].

[20] “Alexa Fluor™ 350 Phalloidin,” *Thermo Fisher Scientific - US*. [Online]. Available: https://www.thermofisher.com/order/catalog/product/A22281?us&en#/A22281?us&en. [Accessed: 09-Mar-2021].

[21] J. Swift and D. E. Discher, “The nuclear lamina is mechano-responsive to ECM elasticity in mature tissue,” *Journal of Cell Science*, 15-Jul-2014. [Online]. Available: https://jcs.biologists.org/content/127/14/3005. [Accessed: 15-Mar-2021].

ACADEMIC VITA

Abby Riggio

EDUCATION

The Pennsylvania State University — **University Park, PA**
Schreyer Honors College — *Anticipated: May 2021*
College of Engineering | Bachelor of Science in Biomedical Engineering

WORK EXPERIENCE

Department of Biomedical Engineering — **University Park, PA**
Undergraduate Grader — *Jan 2021-Present*
- Serve as liaison between professor and students
- Responsible for grading assignments each week

Pediatric Alliance — **Pittsburgh, PA**
Intern — *May 2017-Aug 2017*
- Wrote and published press releases regarding children safety

SERVICE AND LEADERSHIP

THON — **University Park, PA**
Hospitality Captain: Captain Meals — *July 2020-Present*
- Coordinate food and beverage donations
- Lead a committee of 23 student volunteers

Hospitality Committee Member: Family Relations Chair — *Oct 2018-Aug 2020*

Harmony — **University Park, PA**
Volunteer — *Sept 2019-Present*
- Mentor individuals with disabilities through social skills/acting exercises
- Foster a sense of community between participants and student volunteers

UPMC Hillman Cancer Center — **Pittsburgh, PA**
Volunteer — *July 2019-Present*
- Provide support and meals for inpatients
- Escort patients and visitors to appointments

Women in Engineering (WEP) — **University Park, PA**
Study Group Facilitator — *Jan 2019-May 2019*
- Led a physics study group for ten first year students
- Mentored other women in engineering

Learning Assistant — **University Park, PA**
Chemistry Department — *Dec 2017-May 2018*
- Facilitated learning within a large general chemistry course
- Answered daily questions and led review sessions

SKILLS

Laboratory Techniques
Experience with: DNA/RNA extraction, microscopy, mammalian cell culture

Computer Programs

Solidworks, COMSOL, 3-Matic, Mimics, MATLAB